Sedimentologic and Hydrodynamic Trends Along a Modern Fluvial to Marine Transition Zone:

Mud Deposition in the Lower Waihou River, Aotearoa-New Zealand

A thesis

submitted in partial fulfilment

of the requirements for the degree

of

Master of Science (Research) in Earth Sciences

at

The University of Waikato

by

Ben Roche

THE UNIVERSITY OF
WAIKATO
Te Whare Wānanga o Waikato

2022

Abstract

The fluvial to marine transition zone (FMTZ) is a dynamic environment, subject to a mixture of marine and riverine forcing mechanisms. These processes control deposition of sediments, which can hold valuable natural resources. However, due to the complex process regime, the sedimentary successions from these areas can be difficult to interpret. This study aims to improve depositional models by linking quantified measurements of the active processes to their deposits along the transition zone, using a modern example of these systems, the Waihou River in the North Island of Aotearoa-New Zealand. This study produced three main findings, which are relevant to people researching ancient shallow marine strata: 1) The locus of mud deposition occurs in the middle of the transition zone due the combined influence of depositional and preservational controls. Mixing of marine and freshwater reduces landward, which limits flocculation, and hence, deposition of mud upstream. In contrast, preservation of mud deposits is reduced towards the mouth of the river as a result of faster flow speeds. Midway between these two endpoints is a region where deposition and preservation of mud is the largest within the FMTZ. 2) Fluid mud deposits are poorly preserved in the deepest parts of channels, likely due to the high energy levels in this environment. Nevertheless, our results do not preclude the possibility that significant accumulations may occur in the shallow parts of the cross-channel profile. 3) Mud facies diversity is an indicator of depositional position along the FMTZ. Facies diversity was greatest at the middle observational site, which corresponds to the area that is subject to the most variable process regime. The landward and seaward ends of the transition zone exhibit a greater level of dominance in solely riverine or marine depositional processes, respectively. This study yields new insights into the process-response relationships for mud deposition at the interface of land to sea.

Acknowledgments

First and foremost, I would like to thank my chief supervisor Dr. Andrew La Croix for his continued guidance through a challenging project, and his ability to help me “see the forest form the trees”, which has always been by greatest short coming. My thanks also go out to my secondary supervisor Associate Professor Julia Mullarney. Her efforts behind the computer and out in the field (even the critiques on my field lunches) were noted, appreciated, and learnt from. Together they are the “A” team of supervises, and without their blood, sweat and edits, this would not have been possible.

The data collection for this study was logistically challenging, and thus a great deal of technical help was need. Thanks to the University of Waikato technicians that assisted with the deployment and retrieval of instrument frames; a special thanks must go to Chris Morcom and Warrick Powrie for diving in water with an aroma akin to that of cow pat. I would also like to thank the Thames Harbour Master, Rod Edwards, who assisted in setting navigation marker around each site and who skippered a watch boat for the divers. The coring was conducted from a large barge skippered by Brian Coxhead with help from Nik Weyel; thanks to you both for your hard work and to Sharon Coxhead for liaising with us behind the scenes. Thanks to Kirsty Vincent, Holly Harvey-Wishart and Annette Rodgers for help with lab-based activities such as particle sizing, water sample processing and for advice on the rate at which I should be writing chapters (Annette).

I would like to extend my thanks to the local iwi (Ngāti Maru) for granting us permission to conduct our work, and to Russel Riki for guiding us through the pōwhiri at the Matai Whetu Marae. Russel also helped me practice and improve my pepeha, for which I am most grateful.

My mangers (Chris Morcom, Helen McKinnon, and now Kat Rowe) have always been accommodating, and my colleges extremely understanding, of my absences, for which I am very thankful. It’s finally over, thanks to you all.

To all my friends I have made or held onto over my seemingly never-ending period of study, thank you. Everyone has played a role in helping me get to where I am now, whether it be advice about writing, helping with bathymetry surveys on fishing trips, or giving me grief about not finishing sooner, it has all helped. Specifically, I would like to thank Eva Bonning and McGregor Small (my flatmates), who have had to live with stressed me for a good while, thanks for picking up my slack when I needed it most.

I would like to thank my parents Andrew and Jane Roche for always backing me and my ambitions, it really means a lot. Having you both in my corner through my studies has made the journey that much easier.

Last, and certainly not least, I would like to thank my partner, Kacey Bennett. It's been a rollercoaster, and you've been in the passenger seat the whole way; through the ups and downs you have remained by side. You are always keen to see me do well, even if that means showing some tough love, like pausing "Suits" until I go away and start writing again. Thanks for looking after me in these last few weeks, I'll always remember your contribution to this achievement.

Table of Contents

List of Figures

List of Tables

Chapter 1

Literature review

1.1 Introduction

The fluvial to marine transition zone (FMTZ) comprises an exceptionally diverse and complex set of sedimentary environments that result from the mixing of fluvial waters into a marine basin. Understanding the fluvial to marine transition zone has been an active area of research for several decades, which continues today, as an abundance of natural resources are contained within strata deposited in this zone (La Croix et al., 2019; Mackay & Dalrymple, 2011; Weymer et al., 2020). Process-response relationships between hydrodynamic forcing and resultant sedimentary deposits have provided valuable insights into Earth surface history and evolution at this land-to-sea interface (Dalrymple et al., 2003; Dashtgard et al., 2022; Gugliotta et al., 2017; La Croix & Dashtgard, 2015). However, much work is still needed to characterise the full suite of deposits, and to link deposits to their formative processes. One conspicuous aspect of the sedimentary record where more data are needed, are the mud deposits which accumulate in tidal-fluvial channels, especially since we now know that mud deposits encompass a wide range of depositional environments and conditions (Baas et al., 2009; Mackay & Dalrymple, 2011; Schieber et al., 2007; Schieber & Southard, 2009). Despite the generally high-energy conditions along the fluvial to marine gradient, mud has been shown to be deposited in abundance (La Croix and Dashtgard, 2014; Gugliotta et al. 2020) because cohesive forces caused by high clay concentrations suppress turbulence, and clay grains flocculate which drastically increases their settling velocity (Sutherland et al., 2015). The discovery of this dynamically deposited mud has called for the re-evaluation of rock record interpretations, but first, a better understanding of the depositional mechanisms for mud must be established using modern analogues.

The Waihou River on Te Ika-a-Māui (the North Island of New Zealand) is a small, mud-dominated river system that has built a tidally influenced delta where the freshwater enters the mesotidal Firth of Thames. The system therefore offers an opportunity to observe the deposition of mud, link the deposits to their processes, and to answer the following open research questions:

1) Can dynamically deposited mud be directly observed within a modern sedimentary system and the resultant deposits linked to the flow processes?
2) Can the answer to question 1) be used to constrain depositional position along the FMTZ?

This thesis will answer these questions by pairing oceanographic observations with sedimentological data collected from the channel within the FMTZ of the Waihou River. The thesis comprises three chapters. Chapter one (this chapter) provides an overview of the study area and state of knowledge regarding mud deposition in the FMTZ through a detailed literature review. The review will also set the stage for the study by describing the regional geology and oceanographic setting of the Waihou River. Chapter two is presented in "paper format", in which I describe how data was collected, outline the results, and discuss the findings in the context of previous studies. In Chapter three, I evaluate to what degree this study answered the research questions and outline what future work is needed characterise the study area and expand our understanding of dynamic mud deposition.

1.2 The Fluvial to Marine Transition Zone

1.2.1 Hydrodynamics

The relative contributions of tides, river flow, and waves on hydrodynamics and sediment deposition though the FMTZ vary in a broadly predictable fashion, allowing depositional position within the zone to be approximated (Dalrymple & Choi, 2007). In most tide-dominated systems tidal amplitude will increase landward due the constriction of the cross-sectional area of channels, and then eventually diminish due to bed friction ('hypersynchronous'; (Dalrymple & Choi, 2007)). The point of maximum tidal amplitude corresponds to fastest tidal velocities (Dalrymple & Choi, 2007) (Figure 0.1). Conversely, settings where a funnel shaped geometry is lacking, bed friction becomes more important than the constriction effect and tidal amplitude will decrease as the wave propagates inland (Dalrymple & Choi, 2007).

River flow speeds decrease seaward due to a reducing hydraulic gradient, and often channels may split into distributaries (Dalrymple & Choi, 2007). The effect of tides opposing river flow means that as the riverine water travels towards the sea, tidal effects become greater (Dalrymple & Choi, 2007). The term tidal limit is used to represent the furthest landward

propagation of tides (Dalrymple & Choi, 2007), above which flow is always directed seaward. Downstream of this point, the effects of tides may first be felt by modulation of the seaward velocity followed by complete retardation and then by finally by reversal of flow (Dalrymple & Choi, 2007). The tidal limit can also be impacted by river flow where, during low flow stages, the tidal limit is shifted inland, resulted in tidally modulated deposits within a dominantly fluvial landscape. For these reasons the tidal limit should be thought of as a zone as opposed to a fixed position (Dalrymple & Choi, 2007). The separation of the riverine and tidal flow components means that water may be flowing both landward and seaward within close proximity (Dalrymple & Choi, 2007). Due to shoaling of the tidal wave as it propagates into shallow water, most of these systems are flood dominant, and hence net flow direction is often landward near the mouth of the system and seaward in the fluvial dominated portion. This change produces what is known as the bedload convergence zone (BLC, Figure 0.1) which is where dominantly sand sized bed load material is concentrated due to the convergence of the net transport directions (Dalrymple & Choi, 2007).

Waves may be important in generating local currents and orbital velocities at the bed which impact sedimentation near the mouth of estuaries (Dalrymple & Choi, 2007). As many tidally dominated systems have a funnel shaped morphology, it is possible for waves to propagate some distance inland. The relative importance of waves within any particular system is mostly influenced by the local wave climate, fetch (depending on water depth, and wind directions), and the strength of river flow and tides which also mobilise sediment (Dalrymple & Choi, 2007; Hunt et al., 2016).

The mixing of marine and fresh water along the FMTZ can influence flow structures and resultant depositional products (Dalrymple & Choi, 2007). Stratification occurs in the flow where a marine wedge propagates inland underneath outflowing freshwater due to difference in density (~1000 $kg.m^{-3}$ for fresh water versus ~1025 $kg.m^{-3}$ for marine water); the vertical degree of stratification (from partially stratified to a strong saltwater wedge) is controlled by the turbulence induced by opposing currents at the interface and at surface and bed boundaries. The length of this transitional brackish water region is also dictated by both the river discharge and the intensity of mixing; the region of mixing can range from tens to hundreds of kilometres in length (Dalrymple & Choi, 2007). These regions where freshwater laden with fine suspended material meets the salt wedge are known as the turbidity maximum zone, and suspended sediment concentrations in this zone are strongly influenced

by flocculation which is enhanced by the increase in salinity and flow structure (Dalrymple & Choi, 2007). FMTZs can occur in both estuaries (transgression through time) and deltas (progradation through time). The resultant facies are similar, but their stacking patterns are different, which is important for helping unravel the sedimentary record (Dalrymple & Choi, 2007).

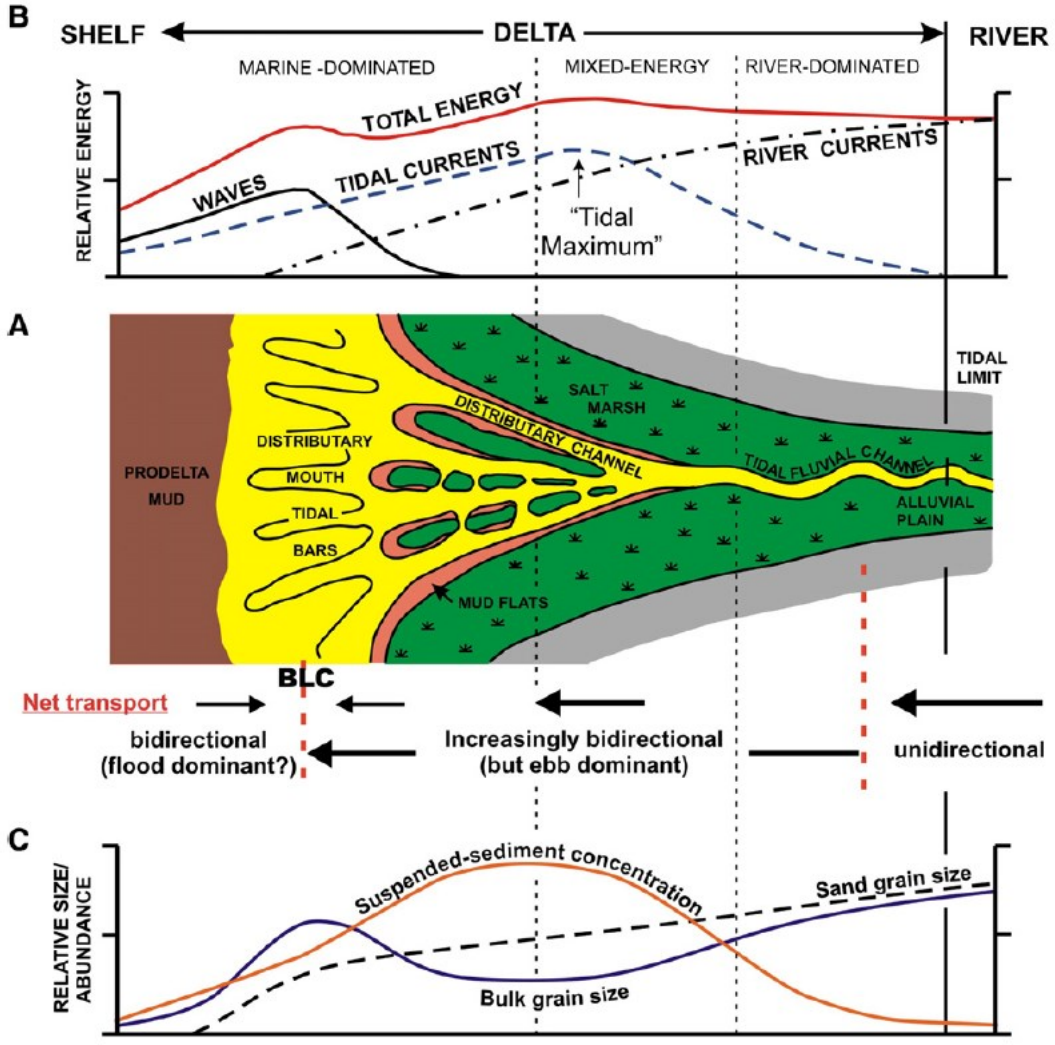

Figure 0.1: Conceptual diagram of the hydrodynamic changes from estuarine to fluvial environment in a tide dominated estuary. Figure from Dalrymple and Choi (2007).

1.2.2 Indicators of depositional position

The position of the turbidity maximum zone can be determined based on systematic changes in the nature of mud deposits in channels within the FMTZ. In the Fraser River Delta, Canada, La Croix and Dashtgard (2014) found that sand bed thickness and proportion are greatest near the inland tidal limit, decrease through the turbidity maximum zone, and then increase again

towards the mouth of the system. The inverse pattern is true for mud beds, which are virtually absent near the inland tidal limit, reach maximum thickness and overall proportion through the turbidity maximum zone, and then decrease in thickness towards the mouth. Sand and mud bed thickness were also found to be the least variable through the turbidity maximum zone (La Croix & Dashtgard, 2014).

Sediment chemistry and palynology can be used as a proxy for depositional position along the FMTZ (Czarnecki et al., 2014; Thornton & McManus, 1994; Wang et al., 2021) (Figure 0.2). Thornton and McManus (1994) investigated the use of sediment chemistry as a mean of determining the source of organic material within the fluvial-tidal transition. Of the methods investigated ($\delta^{15}N$, $\delta^{13}C$ and C/N ratios) only $\delta^{13}C$ proportions gave consistent results that allow the determination of the source of organic matter within the sediments (Thornton & McManus, 1994). High $\delta^{13}C$ values indicted a marine organic source while low values indicted a terrestrial signature (Thornton & McManus, 1994), which was thought to be due to the isotopically distinct marine phytoplankton causing the heavy carbon signature. Czarnecki et al. (2014) also used $\delta^{13}C$ analysis to deduce the source of sediment revealing a similar trend to the study by Thornton and McManus (1994). Both studies compared the sediment source to depositional position along the FMTZ with varying results; Thornton and McManus (1994) found that the marine sediment signature was dominant until approximately the landward limit of the salinity intrusion whereas Czarnecki et al. (2014) only identified marine signatures in deposits seaward of the upper delta plain. These differences could potentially be explained by to the regressive versus propagational nature of the respective study areas. In the same study Czarnecki et al. (2014) related palynological assemblages to depositional position along the FMTZ. Marine influence was measure by the proportion of marine dinocysts relative to terrestrial palynoflora and also the diversity of dinocysts (Czarnecki et al., 2014). It was found that there were no systematic changes in palynological assemblages through the majority of the FMTZ until the region where salinity became stable, causing the relative proportion and diversity of dinocysts to increase (Czarnecki et al., 2014) (Figure 0.2). Based on this evidence, the authors deemed that palynological and geochemical trends are poor indicators of depositional position along tidally influenced deltas and that sedimentological and ichnological data sets provide more robust information (Czarnecki et al., 2014). However, a more recent study (Wang et al., 2021) provided evidence to suggest Sr/Ba ratios extracted using acetic acid (Sr/Ba-HAc) and ammonium acetate (Sr/Ba-NH4A) may be a good alternative

to the other depositional position proxies . Dashtgard et al. (2022) reviewed the used of these indicators on the Fraser River system and found that Sr/Ba-HAc and Sr/Ba-NH4A ratios were the best predictor of sustained marine conditions usable by sedimentologists in ancient strata. However, they noted the caveat that all of the methods tested were significantly impacted by riverine sedimentation, so comparisons should only be drawn between systems with similar riverine influence (Dashtgard et al., 2022).

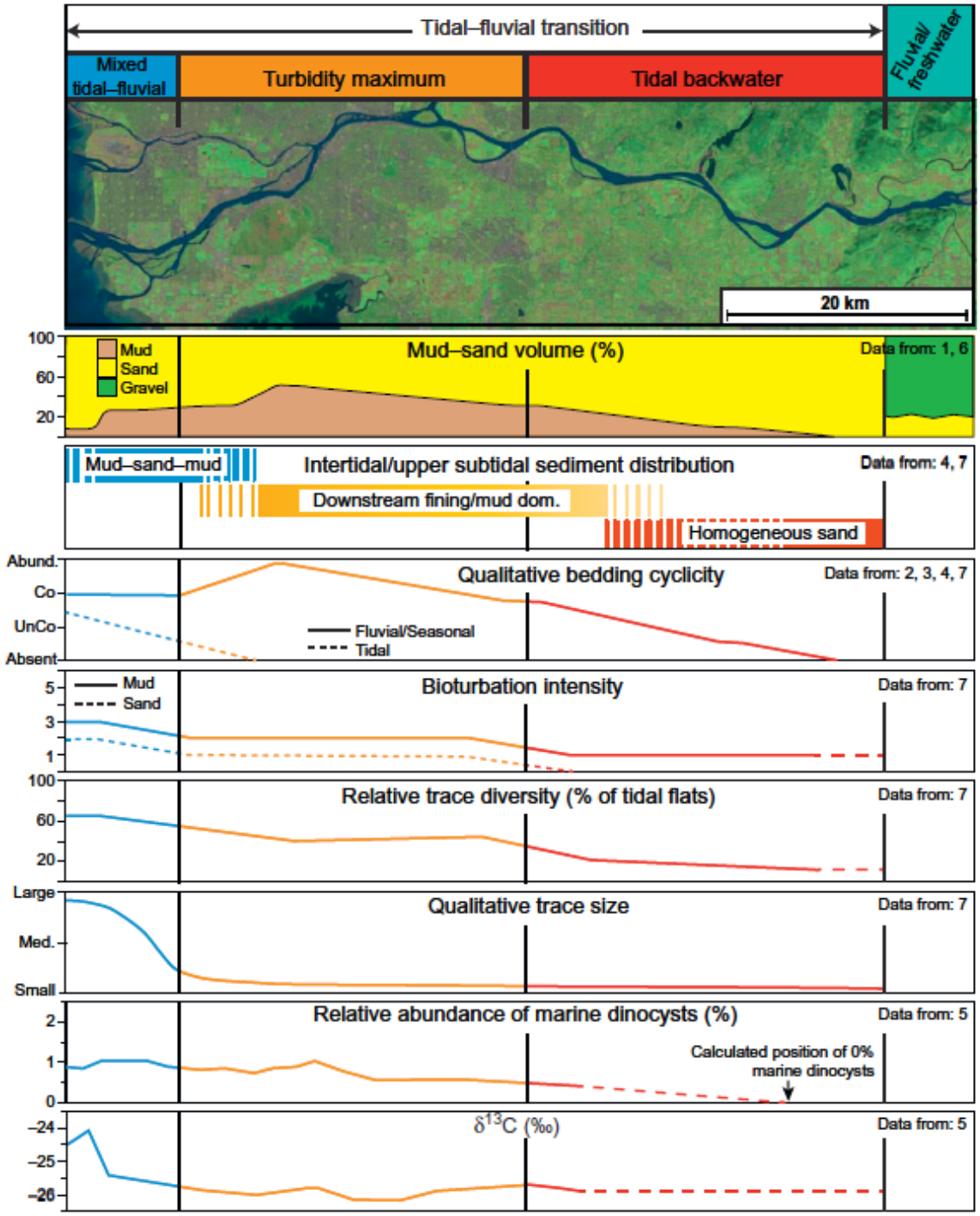

Figure 0.2 Proposed model for depositional trends along channel bars of tidally influenced deltas. Figure from Dashtgard and La Croix (2015).

Physical sedimentary structures are also useful for determining depositional position within the FMTZ (Dashtgard & La Croix, 2015; Gugliotta et al., 2017; La Croix & Dashtgard, 2015). Muddy current ripples and graded current ripples are bedforms that fine from crest to trough; these form due to turbulence dampening in the lee side of ripples due to elevated SSC (Baas & Best, 2008; Mackay & Dalrymple, 2011) and by the flocs behaving as pseudo-sand grains allowing the formation of typically traction-generated structures (Schieber & Southard, 2009). Muddy current ripples are most common within the vicinity of the turbidity maximum zone (TMZ), whilst graded current ripples are more prevalent near the mouth of the system. Within the freshwater reach of the systems, mud deposition is negligible (Dashtgard & La Croix, 2015; La Croix & Dashtgard, 2015). Heterolithic bedding patterns also change in a predictable manner along the FMTZ, while lenticular beds are most common within the turbidity maximum zone and wavy or flaser beds dominate close to the mouth due to the fast tidal currents (La Croix & Dashtgard, 2015) (Figure 0.2).

1.2.3 Ichnology

Due to variability in water salinity, flow conditions, and subaerial exposure (within intertidal regions), the FMTZ is a very dynamic and physiologically stressful environment for burrowing animals to live (Dalrymple & Choi, 2007; La Croix et al., 2015). Because of these ecological conditions, there is a much lower diversity in trace fossil assemblages (Gingras et al., 1999; La Croix et al., 2015). The majority of animals living within the region employ opportunistic behavioural adaptations that allow them to survive, such as rapidly colonising sediment during ideal conditions, living within the sediment as opposed to on the surface, and adopting novel feeding techniques such as deposit mining or suspension feeding (Dalrymple & Choi, 2007). La Croix et al. (2015) summarised the finding of several studies of the bioturbation trends across the fluvial to marine transition within intertidal sediments; they found that bioturbation diversity, intensity/density and burrow size all decreased with growing freshwater influence as seen in Figure 0.3. Hauck et al. (2009) also noted these trends and added that, although these trends can be strongly correlated with patterns in salinity, the

patterns are likely modulated by turbidity and other stressors produced by these transitional environments.

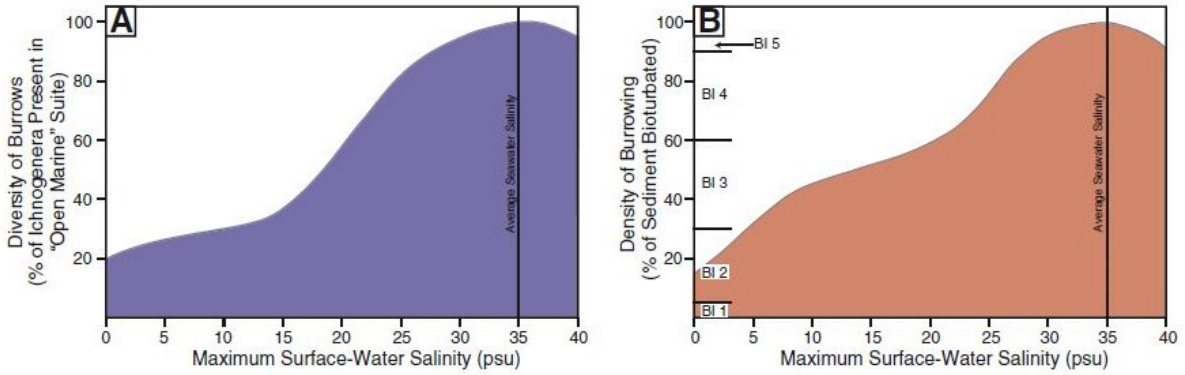

Figure 0.3 Conceptual model of trace fossil assemblage diversity (A) and burrow density (B) for intertidal sediments through a gradient of surface salinities. This model is based on data from five different FMTZ transitional systems. The divisions in panel B show the different bioturbation indices for reference. Figure from La Croix et al. (2015).

1.3 Muddy Flows and Their Depositional Products

1.3.1 Flocculation of mud and its significance in the rock record

Macquaker and Bohacs (2007) noted that mud deposition is more complex than previously thought and that the work by Schieber et al. (2007) expels the preconceived notion that muds are only deposited within low energy systems. It has been shown that flocculation occurs over a broad range of salinities (from as low as 0.6; (MacDonald & Mullarney, 2015)) with the most prevalent flocculation occurring around 10 PSU, which is characteristic for the salinity in the zone of brackish water mixing within modern estuarine systems (Sutherland et al., 2015). Within freshwater systems, it is expected that fine material will settle at the Stokes settling velocity, whereas material that is flocculated can settle at considerably faster velocities (Sutherland et al., 2015). Sutherland et al. (2015) showed that clay suspended in fresh water can take tens of hours to settle to the base of a 10 cm deep tank, as opposed to clay within saline suspension that can fall out solution with tens of minutes. The mechanism causing flocculation is the interaction between Na and Cl ions in marine water with the charged surfaces (and ends of) of clay particles, thus eliminating repulsive forces that prevent electrochemical attraction between clay particles (Sutherland et al., 2015). Research by Schieber et al. (2007) showed that even at high flow velocities (0.2-0.3 $m.s^{-1}$) these flocs can drop out of suspension much like sand grains to form mud ripples when muddy flows are

sustained for a period of time. It was later determined that traction transport of mud to form ripples on the bed was not solely confined to terrigenous muds and that similar structures can be formed by carbonaceous muds (Schieber et al., 2013). Such a finding suggests that sediment chemistry is less important than suspended sediment concentration in controlling mud deposition (Schieber et al., 2013). Another factor influencing mud deposition and bedform morphology is the presence of organic polymers and proteins ('extracellular polymeric substances'; EPS) produced by communities of benthic microalgae that act to bind and stabilise sediment (Baas et al., 2019). Only ~3% EPS is required to alter the migration and development of bed forms. It has been shown that EPS within the sediment matrix plays perhaps the most important control on bedform morphology as opposed to the high-volume biofilm at the sediment-water interface (Malarkey et al., 2015).

The structure of clay rich flows was investigated in detail by Baas and Best (2002). They segregated flow types based on the vertical profiles of turbulence intensity and the development of shear layers as a consequence of increasing the cohesive force acting within the flow (as a result of increasing clay concentration). They classified flows into turbulent flow, transitional flow, and laminar or plug flow. The transitional flow separates Newtonian and non-Newtonian flow behaviour, which is a result of electrostatic bonding between clay particles dampening turbulence. The analysis of possible flow types was then expanded on by Baas et al. (2009), who subdivided the transitional component into three separate flow types to better characterise the development of the laminar plug (Figure 0.4). Turbulent flow is associated with the lowest concentrations of clay, which has the same structure as flows when no clay is present, meaning that turbulent intensities decrease away from the bed (Baas et al., 2009). Turbulence-enhanced transitional flow captures the increase in overall turbulence due to the early stages of internal shear layer development (Baas et al., 2009). Within lower transitional plug flow, the laminar plug is developed and by upper transitional plug flow the plug is well developed atop an internal shear layer (Baas et al., 2009). Finally, quasi-laminar plug flow is when a plug of clay rich fluid rides over the bed above a thin layer with a very large vertical velocity gradient (Baas et al., 2009).

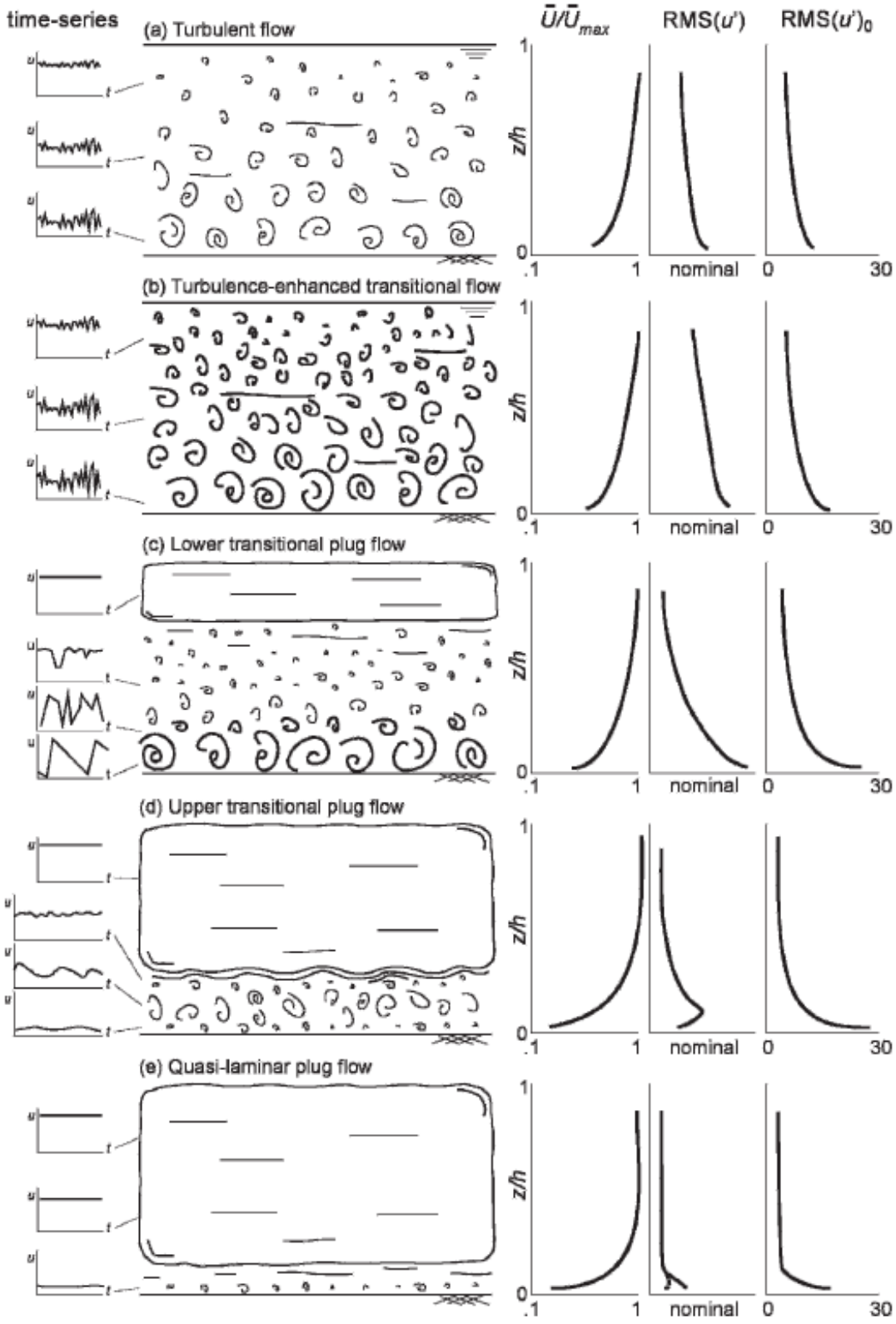

Figure 0.4 Conceptual diagram of the five main clay rich flow types as defined by Baas et al. (2009). Figure from Baas et al. (2009).

These conceptual models of deposition have been applied to ancient sedimentary systems to interpret past flow conditions and several mudstone facies types have been determined

based on these comparisons (Mackay & Dalrymple, 2011). Examining mud bed types in the Cretaceous Bluesky Formation in the Western Canada Sedimentary Basin, Mackay and Dalrymple (2011) found four distinctive mechanisms for mud deposition (Figure 0.5): (1) thin unstratified mudstone which is thought to represent slow settling of particles out of the water column at slack water; (2) thick structureless mud stone which is thought to be the product of fluid muds freezing to the bed under quasi-laminar or unstable plug flow. These beds have sharp basal contacts and commonly have flame structures or other soft sediment depositional features in the upper contact due to the high water content of the material; (3) low-angle cross stratified mudstones which are interpreted to occur under turbulent to transitional plug flow which is indicated by the presence of sets of traction-generated current ripples that can be graded down ripple (thus turbulence is not fully suppressed); and, (4) planar-laminated mudstones which are characterised by very fine alternating laminations that are thought to be due to high frequency alteration in shear stress beneath the mobile fluid mud layer under transitional to quasi-laminar plug flows. These bed types can all be preserved within decelerating flow successions (Figure 0.6). The initial SSC and flow speed will dictate the resultant succession as illustrated by scenarios A, B and C in Figure 0.6.

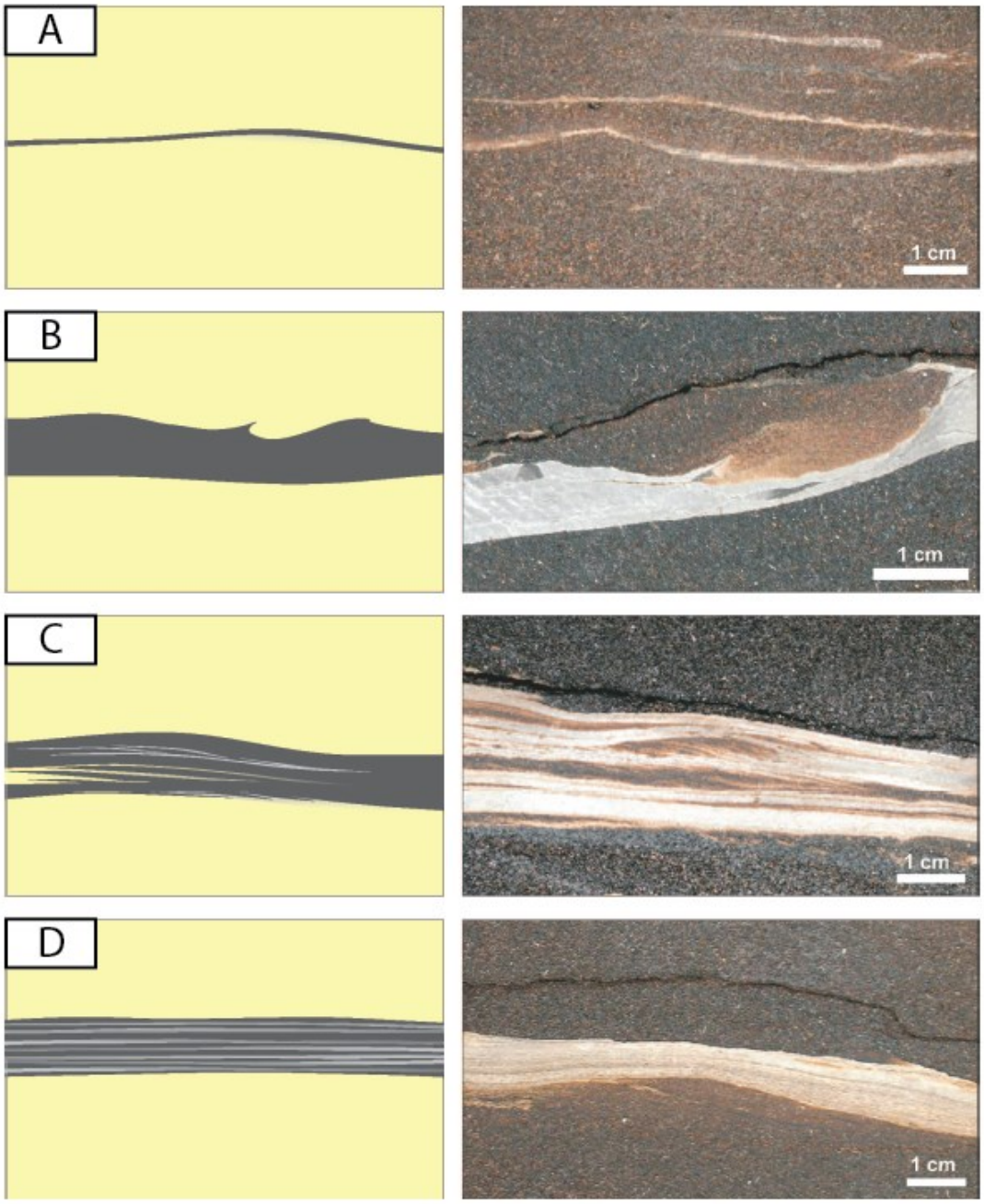

Figure 0.5 Mudstone facies from the Bluesky Formation. Panel A shows and example of thin structureless muds. Panel B shows thick structureless muds with loading structures at the upper contact. Panel C shows current rippled muds, while Panel D shows planar laminated muds. Figure from Mackay and Dalrymple (2011).

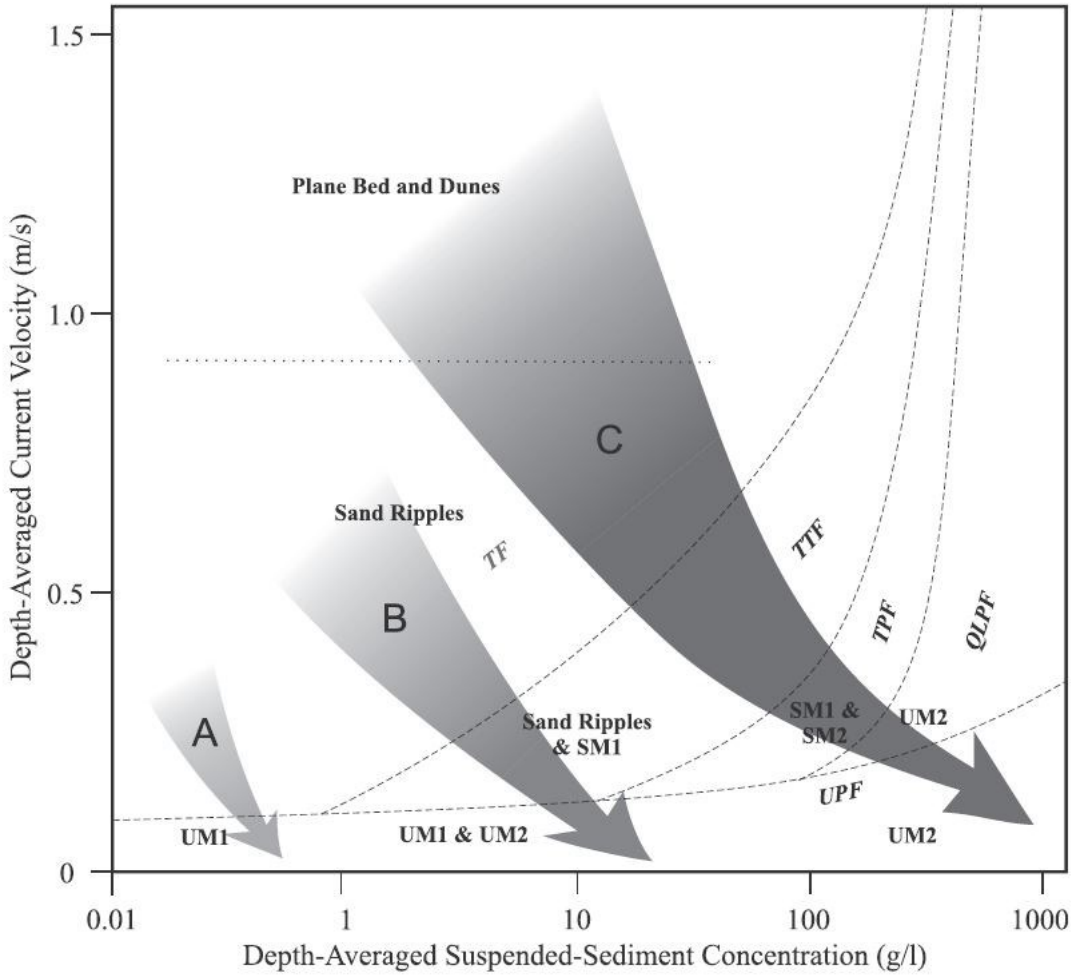

Figure 0.6 Stability field diagram showing possible decelerating flow paths (A, B and C). Figure from Mackay and Dalrymple (2011).

1.4 Waihou River

1.4.1 Regional setting and pre-Holocene sedimentation

The Waihou River is situated within an active rift system that is a sediment depocenter due to long term rapid subsidence of the basin floor (Hochstein et al., 1986; Hochstein & Nixon, 1979). The rift structure is known as the Hauraki Rift, which is approximately 25 km across and stretches from the Taupo Volcanic Zone (TVZ) into the outer Hauraki Gulf over a distance of ~220 km (Hochstein et al., 1986). Neogene andesite-dacite volcanics of the Coromandel Group and rhyolites of the Whitianga Group border the Hauraki Rift along the Coromandel-Kaimai Mountain Range to the east, and Jurassic metagreywackes of the Hunua-Hapuakohe rim the rift in the west (Naish et al., 1993; Skinner, 1986) (Figure 0.7). The Hauraki Rift has a fault angled depression on the western margin, and a half-graben on the east, which are

separated by a median horst (Hochstein & Nixon, 1979) (Figure 0.8). These depressions have been partially infilled by non-marine Tertiary sediments to a depth of 2-3 km and subsequently by approximately 0.7 km of unconsolidated Quaternary material (Hochstein et al., 1986).

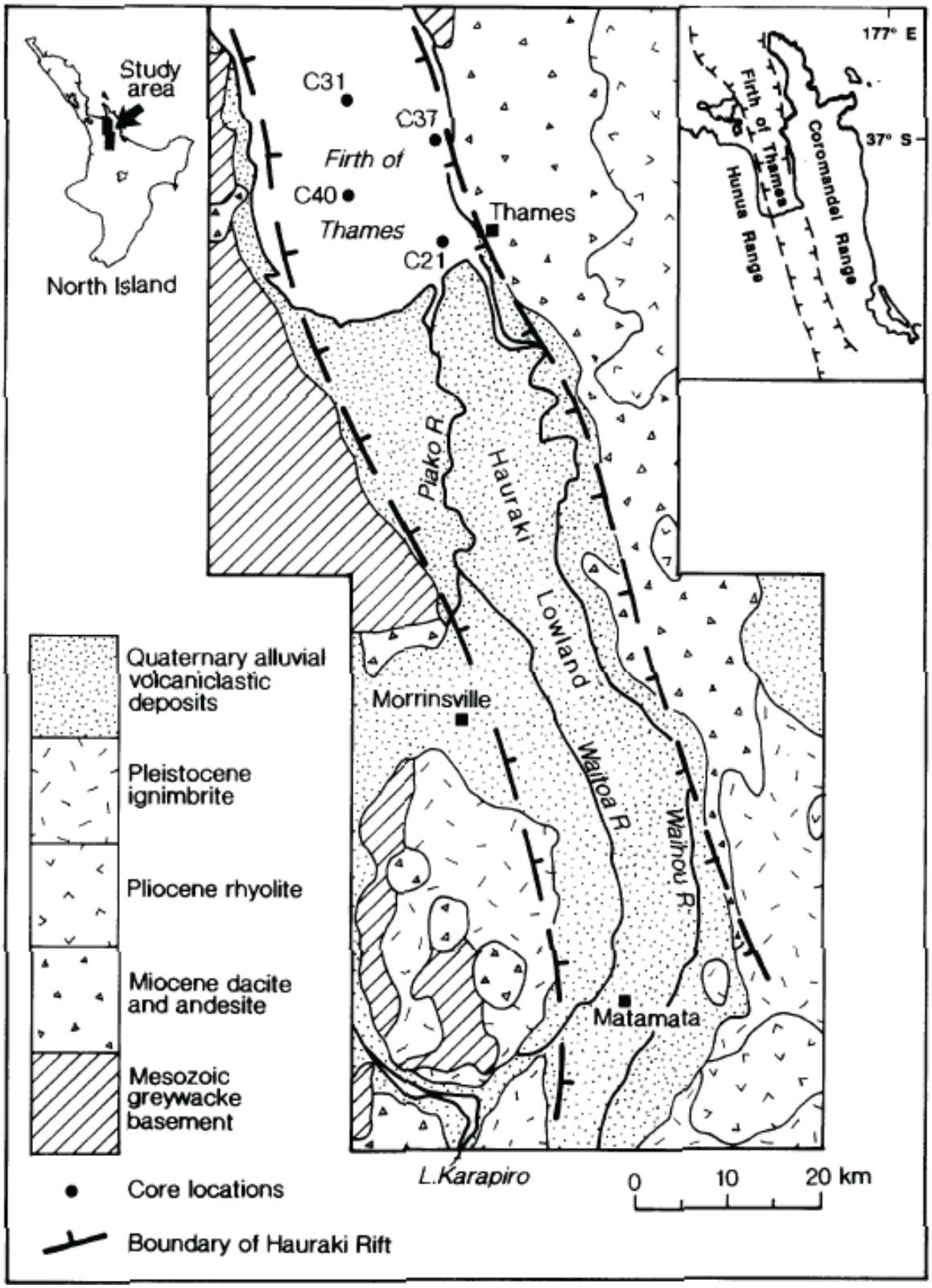

Figure 0.7 Simplified geological map of the Hauraki Rift. Figure from Naish et al. (1993).

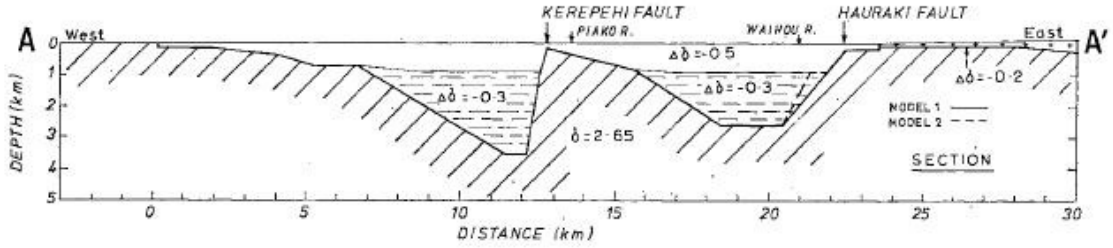

Figure 0.8 Structure of the Hauraki Rift. Figure from Hochstein and Nixon (1979).

Late Pliocene and Pleistocene sedimentation within the rift and rift margins was dominated by emplacement of ignimbrites and their erosional products (Houghton & Cuthbertson, 1989; Leonard et al., 2010). The Waiteriki Ignimbrite outcrops north of the Mamaku Plateau along the Kaimai Range while Pakaumana Group Ignimbrite has been mapped west of Matamata across a large area of the Hauraki Plains (Houghton & Cuthbertson, 1989; Leonard et al., 2010). Mamaku Plateau Formation ignimbrite sheets buried the southern portion of the Hauraki Rift, and these comprise the rocks that underlie the head waters of the Waihou River (Shane et al., 1994; White et al., 2004). Over the last 100,000 years (late Pleistocene to present) the Waikato River switched courses at least four times between the Hamilton Basin and the Hauraki Lowlands, laying down extensive deposits of the Hinuera Formation (Hogg et al., 1987; Manville & Wilson, 2004). The Hinuera Formation is exposed over a large proportion of the plains south of Waitoa (Figure 0.9 provides geographic reference) and overlies the Puketoka Formation which originally filled the rift (Manville & Wilson, 2004).

Figure 0.9 Geographic map showing the settlements within the Hauraki depression.

1.4.2 Holocene sedimentation

During the Holocene (12,000 years ago to present), sedimentation in the Hauraki lowlands was dominated by the reworking and transport of material by the two main river systems (Waihou and Piako Rivers) and to the deposition of material during the mid-Holocene marine transgression (Newnham et al., 1995). Newnham et al. (1995) summarised the formation of the Kopuatai Bog and the marine transgression that resulted in deposition of the Holocene sediments over the northern part of the Hauraki Plains (Figure 0.10). This involved the rise of relative sea-level to its maximum position before 6050 ±110 years before present (De Lange, 1989), after which point, relative sea level fell, depositing deltaic and estuarine sediments over a large portion of the Northern plains (Newnham et al., 1995). As the shoreline receded over the plains in the late Holocene, the peatlands that originally formed within paleochannels upon the Hinuera surface expanded; these peatlands now comprise a large proportion of the north-western plains (Newnham et al., 1995) (Figure 0.10).

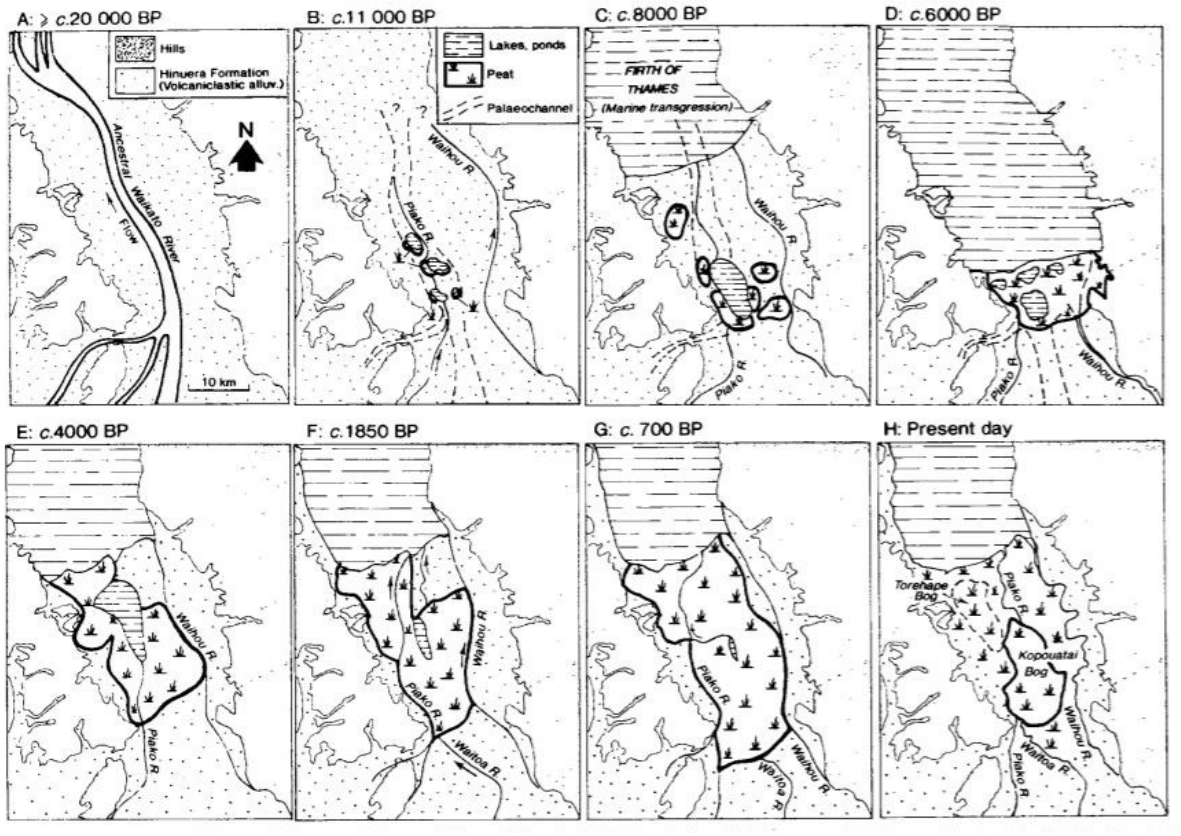

Figure 0.10 Late Pleistocene and Holocene development of the Hauraki Plains and the Kopuatai Bog. Figure from Newnham et al. (1995).

The recession of the Firth of Thames shoreline over the late Holocene was likely a combination of eustatic sea level fall and progradation of the Holocene mud wedge into the ancestral firth (Dougherty & Dickson, 2012; Schofield, 1960; Woodroffe et al., 1983). Through

studying the Miranda chenier plain, Schofield (1960), Woodroffe et al. (1983) and Dougherty and Dickson (2012) deduced that sea level dropped between 2.1 and 0.7 m from c. 4000 YBP to c. 1000 YBP, after which sea level remained at its present level.

1.4.3 Anthropogenic alteration of the Waihou River and Firth of Thames

1.4.3.1 Dredging, stop banking, and channel rearrangement

The Waihou River has been extensively modified since the 1800s through channel works, flood control measures, and changes in land use of the drainage basin. In the early 1900s severe flooding of both the Ohinemuri and Waihou rivers caused extensive property damage in the low lying settlements, which was exacerbated by the government declaring the Waihou and Ohinemuri rivers as sludge channels (Clement et al., 2017). This declaration permitted mining contractor operating in the Karangahake Gorge and around Waihi to release untreated mine tailings into the Ohinemuri River, resulting in aggradation of the river bed (Watton, 1995), and constriction of the river. This constriction likely contributed to the 1907 flood, which deposited mine tailings over a large area of the floodplains close to Paeroa (Figure 0.11).

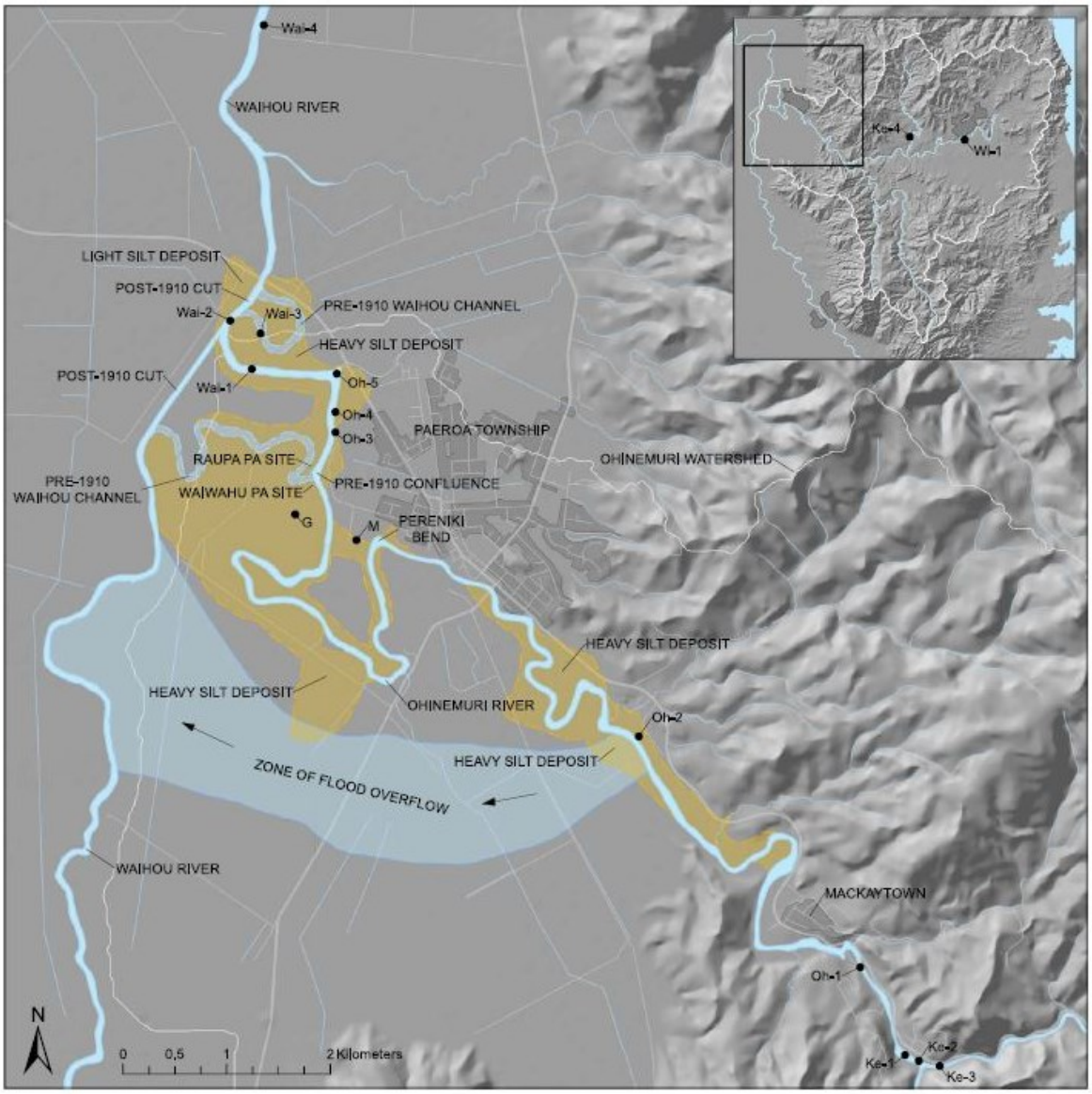

Figure 0.11 Overflow zone of 1907 flood and areas of post flood silt deposits (yellow) near Paeroa. Also shown are channel rearrangements from the Waihou valley flood protection scheme. Figure from Clement et al. (2017).

The Waihou Valley Scheme, as it was later known, was the government's response to the flooding, it involved 10 million cubic meters of earthworks to protect the low-lying settlements of Thames, Paeroa, and Te Aroha. The flood protection scheme involved building of extensive stop banks that encompasses the entire tidal portion of the river, as well as significant channel works, flood gates and pump stations (Watton, 1995). The stop banks were constructed from material dredged from the channel using large floating suction dredges and steam powered Rushton draglines with large (1.1 m^3) buckets (Watton, 1995). There were also several channel rearrangements around Paeroa that aimed to cut out meander bends

and fast track flood waters away from the township (Clement et al., 2017; Watton, 1995) (Figure 0.11).

1.4.3.2 Mining activities upriver from the Firth of Thames

Large quantities of coarse-grained sand from the bed of the Waihou River were mined for use in concrete manufacturing plants located in Auckland ((AJHR), 1921). This mining was done largely unsupervised until the decision by the river commission to direct these mining efforts in a way that could improve channel navigability ((AJHR), 1921).The impact of these sand mining activities on the sediment column within the lower Waihou River remains unknown, but from a process-sedimentological standpoint it may be irrelevant due to the extractive nature of the activities.

1.4.4 Modern sedimentation and sediment dispersal

The Waihou River is the dominant source of sediment to the Firth of Thames where most of the sediment is ultimately retained (Healy, 2002; Pritchard et al., 2015). Griffiths and Glasby (1985) have estimated the annual sediment yield of the Waihou River to be 343000 t/y while Hicks et al (2011) estimated it to be 160000 t/y. Once sediment arrives in the Firth, hydrodynamic modelling has shown that in calm conditions the sediment settles out of the decelerating plume and is not transported more than approximately 2 km from the mouth. Even under storm conditions very little sediment leaves the firth, with most of it being distributed around the southern region and/or along the gravel deltas of the western margin (Healy, 2002; Pritchard et al., 2015). A substantial portion of sediment is also trapped in the mangrove forests lining the Waihou River banks and lower firth (owing to enhanced vegetation-induced friction, which have expanded rapidly over the last 60 years (Horstman et al., 2018; Vundavilli et al., 2021). Sediment transported by both of the rivers that feed the lower Waihou River (Ohinemuri River and Waihou River) is predominantly volcanic glass, which is similar to the sediment composition when the river debouches into the Firth of Thames; the only major difference in sediment composition is that some of the volcanic glass weathers to smectite (Naish et al., 1993) (Figure 0.12).

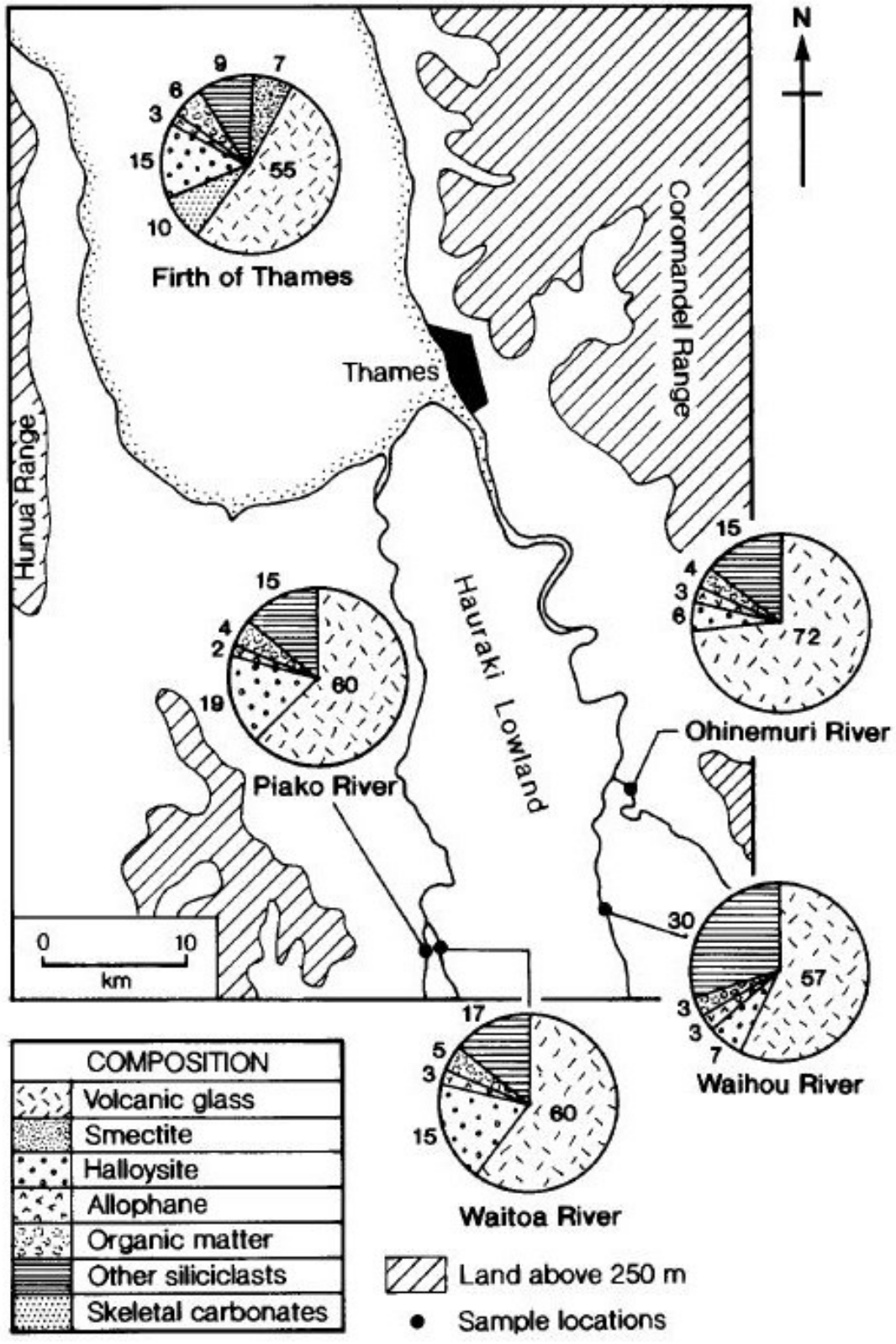

Figure 0.12 Composition of sediment transported by the major rivers on the Hauraki Plains and the composition of sediment within the Firth of Thames. Figure from Naish et al. (1993).

Boehnert et al. (2020) studied sedimentation rates in the south-eastern Firth of Thames and found that sediment accumulation has increased fourfold since the arrival of humans in New

Zealand (ca. 1350 AD). The increase in the rate of sediment accumulation is considered to be largely a product of deforestation and land use change within the catchments. Another factor that may influence the rates of sediment delivery to the Firth of Thames is the artificial confinement of the river through flood protection works, reducing the area available for deposition on the plains, and effectively flushing sediment to the coast. Comparison of three surveys of the Lower Waihou River and adjacent tidal flats near the river mouth provided estimates of sedimentation over the 40-year period leading up to 1919. The calculated volume was 7 million m^3 of sediment deposited in the lower Waihou River and 37 million m^3 in the southern Firth of Thames (Swales et al., 2008).

1.4.5 River flow and tides in the lower Waihou River

The study area for this thesis, within the tidally influenced portion of the Waihou River, means that both tides and river flow (and their interactions) are important controls on sedimentation. The Firth of Thames is a mesotidal estuarine embayment (spring and neap tidal ranges are 2.8 m and 2.0 m, respectively) occupying an area of approximately 800 km^2 (McBride et al., 2016). Water levels of the lower Waihou River are tidally modulated for up to ~35 km along the river due to the low bed gradient, while the intrusion of a saltwater wedge was modelled by McBride et al. (2016) to propagate only 16 km inland.

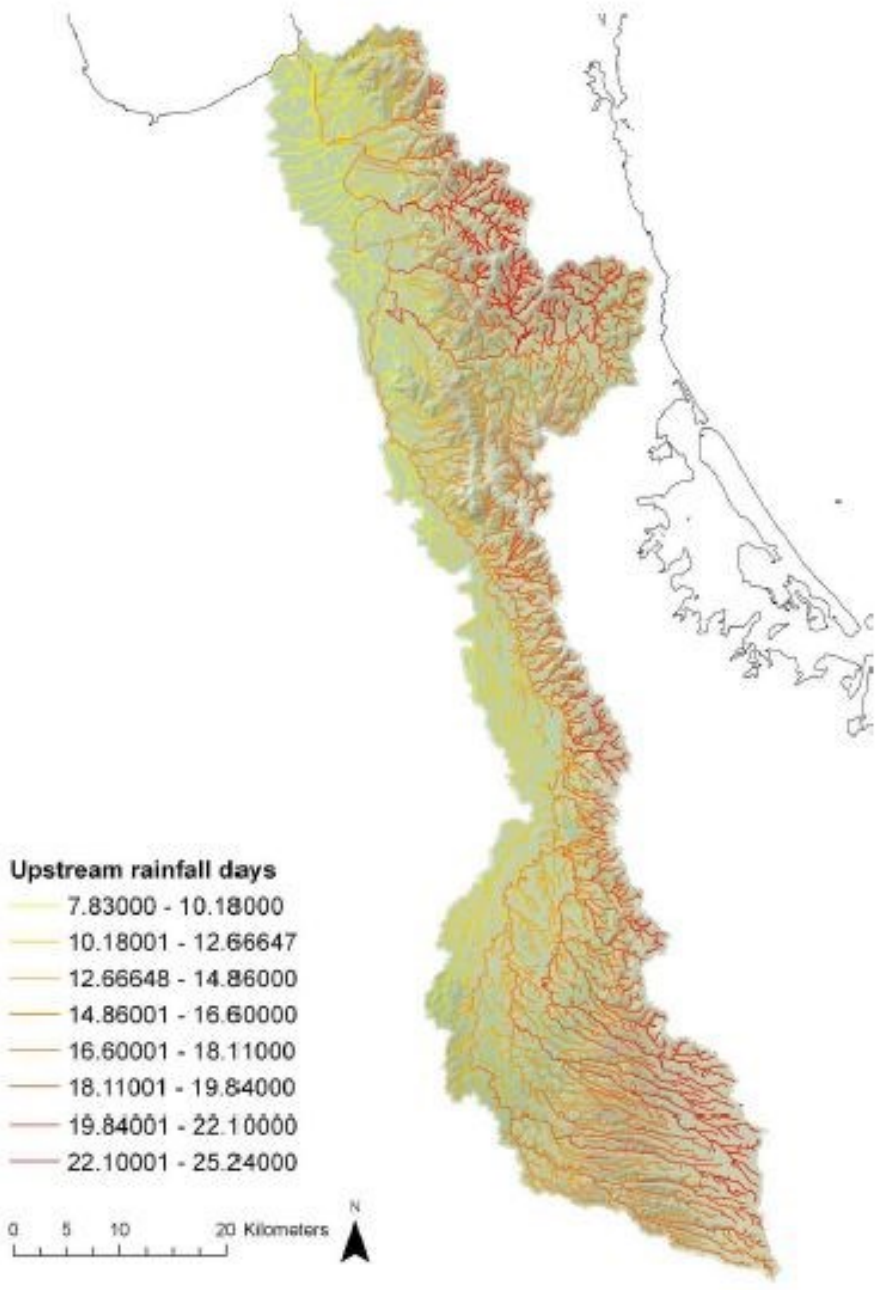

Figure 0.13 Upstream rainfall days greater than 25mm across the Waihou catchment. Figure from Franklin and Booker (2014).

Sediment supply through rivers in New Zealand is controlled to a large extent by episodic, orographically induced, rainfall events leading to pulses of sediment being delivered to the coast (Franklin & Booker, 2014). It is likely that this delivery mechanism is also dominant in the study area based on the distribution of high rainfall days through the Waihou River drainage basin (Franklin & Booker, 2014) (Figure 0.13). Mean daily discharge below the

confluence of the Ohinemuri and Waihou rivers is 52.53 m^3s^{-1} (combining flow data from each river above the confluence), but the flow regime is far more complex (Franklin & Booker, 2014). Flow in the lower catchment of the Waihou River is a combination of base flow from the upper catchment superposed on the flashy flow regime of the steep streams draining the Coromandel-Kaimai Mountain Range, delivering pulses of sediment during rainfall events (Franklin & Booker, 2014).

1.5 Summary

From its source in the Blue Springs on the central North Island of New Zealand, the Waihou River flows northwest over the Hauraki Plains and debouches into the Firth of Thames. The Hauraki Plains have been built within the active Hauraki Rift, which since the Tertiary has been infilled by a 3 km thick succession of sediments and rock predominantly comprising ignimbrites and their erosional products. The Coromandel-Kaimai Mountain Range runs along the eastern side of the Waihou River from which several tributaries feed into the Waihou supplying eroded andesite and rhyolite from the Coromandel and Whitianga groups, respectively. However, most of the sediment transported through the Waihou River is volcanic glass sourced from the Mamaku Plateau ignimbrites. The sediment leaving the mouth of the river is, by and large, retained within the Firth of Thames and is incorporated into the southern mudflats and mangrove forests, or is dispersed across the gravel deltas of the Eastern margin. Although sedimentation within the Waihou River and Firth of Thames has been well studied, including the flood plains and mudflats, there is a dearth of information pertaining to sedimentation within the active river channel and its FMTZ. Despite extensive historical river alteration near Paeroa, much of the lower Waihou River within the study area has been relatively unaltered by humans, except for the construction of stop banks to control floodwater, making this an ideal study area to observe mud deposition and link it to sedimentary processes.

Although sedimentation across the FMTZ has been study widely, most of the trends in sedimentary characteristics have been defined using intertidal case studies. Data from this study will not only address the gap in knowledge about the sedimentology of the lower Waihou River but will also contribute to expanding or refining facies models for channel sediments across the FMTZ overall. It is now known that mud deposition does not only occur in quiescent sedimentary environments through passive particle settling, but it can also occur

within energetic settings due to turbulence damping and flocculation of suspended clays. The structure of muddy flows and flocculation processes have been well documented in flume studies where conditions are idealized, and on that basis these deposits are readily interpreted in the rock record. Perhaps the single largest contribution of this thesis is that, in the absence of other modern analogues, it combines process and depositional data to show a variety of mud depositional styles that hitherto have had no natural examples. The examples contained within this thesis are a world first and are significant step forward in building mud depositional facies models.

Chapter 2

Sedimentologic and Hydrodynamic trends along a modern fluvial to marine transition zone: Mud deposition in the lower Waihou River, Aotearoa-New Zealand

2.1 Introduction

One of the most complex and dynamic sedimentary environments on Earth lies at the land-sea interface within the fluvial to marine transition zone (FMTZ) of rivers (Dalrymple & Choi, 2007). In the FMTZ, tides modulate river flow, marine water is forced landward up channels, and a mixing zone is formed. The corresponding changes in currents and water salinity on hourly, daily, and seasonal times scales manifest in complex sedimentation patterns that are collectively unique to the FMTZ (La Croix & Dashtgard, 2015). Sedimentary deposits from the FMTZ are significant because the stratigraphy holds important information about present and past Earth's surface conditions (Dalrymple & Choi, 2007), and the deposits are known to contain economic accumulations of natural resources (La Croix et al., 2019; Mackay & Dalrymple, 2011; Weymer et al., 2020).

Despite the fact that the sedimentary characteristics of the FMTZ have been investigated previously (Dalrymple et al., 2003; Gugliotta et al., 2017; La Croix & Dashtgard, 2015), most studies have emphasized *either* the hydrodynamic processes (Wu et al., 2022), *or* the sedimentary deposits (Mackay & Dalrymple, 2011). There are currently no studies that link quantitative measurements of flow parameters to the resultant sedimentary deposits within modern depositional systems. This decoupled state of knowledge has left depositional models for the FMTZ incomplete because process-response linkages are not founded in specific case-studies of modern analogues.

One conspicuous feature of deposits that accumulate along the FMTZ is a general abundance of mud. Traditionally these mud deposits are interpreted to represent gravitational settling during slack water periods (McCave, 1970; Potter et al., 2005). However, flume studies have demonstrated that mud deposition can occur under a wider range of conditions than

previously thought, including at fast flow speeds (Baas & Best, 2002; Schieber et al., 2007; Schieber & Southard, 2009), opening up the possibility that mud can accumulate during any phase of the tidal cycle in river channels within the FMTZ. This possibility brings about a need to further examine mud deposition within modern systems with the aim of directly linking sedimentary process with depositional response to improve depositional models within these complex environments.

This study seeks to resolve knowledge gaps regarding mud deposition across the FMTZ by linking hydrodynamic measurements with contemporaneous sediments in the tidally influenced lower Waihou River, New Zealand. The data reveals crucial insights into the relationship between the gradient in flow processes and the signal which is manifested in the associated sediment characteristics. These results fundamentally advance our understanding of mud accumulation in channels along the river to marine gradient.

2.1.1 Waihou River and the Hauraki Depression, New Zealand

The Waihou River has a mean daily discharge of 52.53 m^3s^{-1} (calculated by combining discharge values for Waihou and Ohinemuri rivers above their confluence near Paeroa) and it drains both steep forested area and low-lying plains used extensively for agriculture (Franklin & Booker, 2014). Base flow, derived from springs in the Waihou River's headwaters, constitute a relatively high proportion of river discharge. Quick-flow provided by steep tributaries that drain the Kaimai-Coromandel Ranges is also another significant contributor to river flow (Franklin & Booker, 2014). Approximately 0.16 Mt of sediment is exported from the Waihou River mouth into the Firth of Thames each year (Hicks et al., 2011). The majority of sediment consists of volcanic glass derived from erosion of ignimbrite in the upper catchment (Naish et al., 1993). A large proportion of this material gets retained within the Firth of Thames, and is deposited upon the Firth's southern mudflats, mangrove forests, or along the eastern margins (Pritchard et al., 2015). In the lower Waihou River, tidal modulation of river level occurs up to approximately 35 kilometers from the river mouth and marine water has been estimated to incur to 16 km up river (McBride et al., 2016). For this reason, the location of the study sites were chosen to characterize the gradients in depositional process and sediment characteristics across the mainly brackish-water part of the system (Figure 2.1).

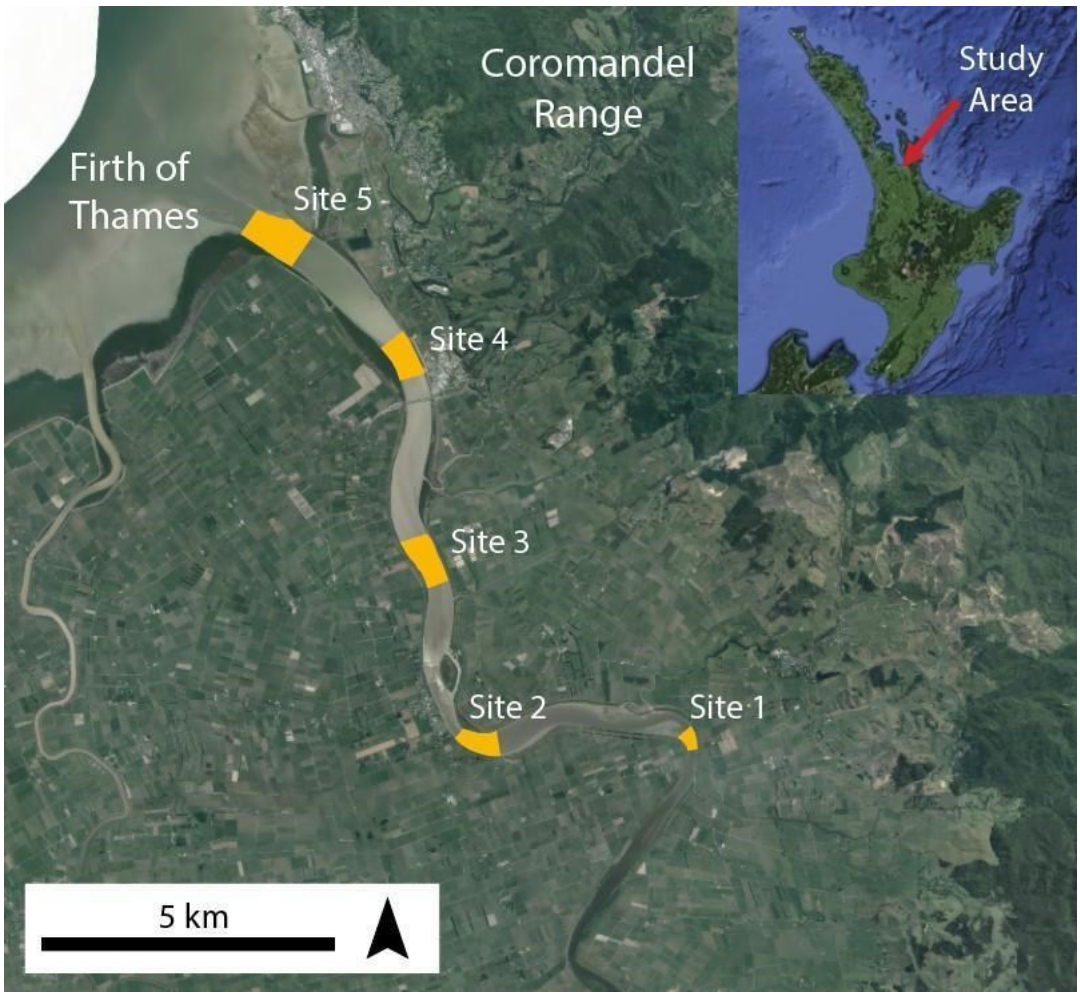

Figure 2.1 Location of the study area, including the five sites chosen for instrumentation and coring along the FMTZ of the Waihou River, North Island, Aotearoa-New Zealand

2.2 Methods

To characterise both the depositional processes and associated sedimentary characteristics within the lower ~15 km of the Waihou River, oceanographic instrumentation was deployed at five locations for a neap-spring tidal cycle during November 2020. Following deployment of instruments, co-located vibracores were then collected, as well as a suite of surface sediment samples. Prior to deployment of instruments and collection of sediment data, bathymetric surveys were conducted to inform instrument and coring positioning and to put sedimentation patterns in context. Figure 2.2 presents examples of the equipment used to collect the data while Table 2.1 summarises the parameters measured at each site along the FMTZ.

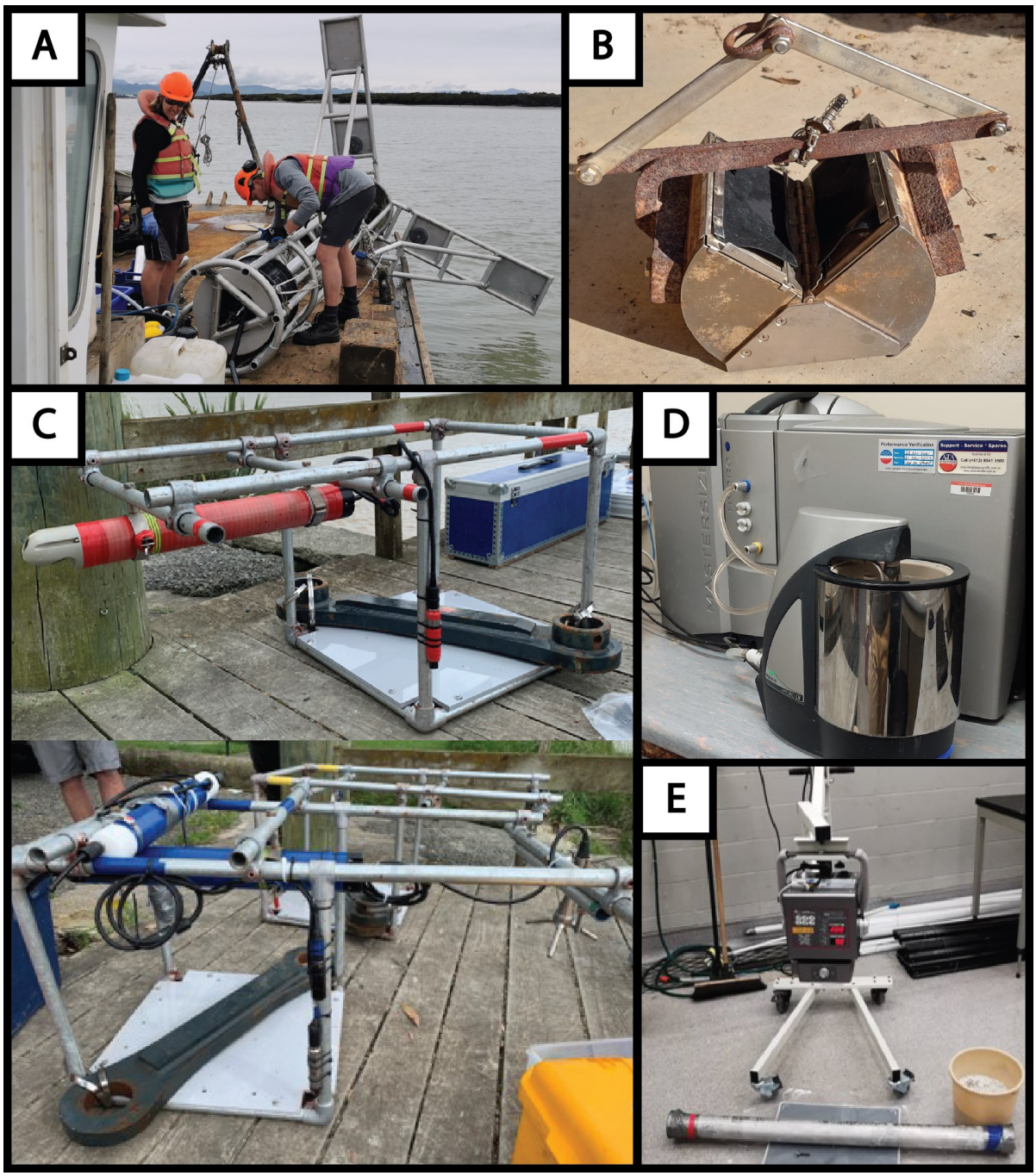

Figure 2.2 Field and laboratory equipment used in this study. A) Vibracoring tower deployed from a barge. B) Ponar grab sampler to collect surface sediment samples. C) Weighted instrument frames with Acoustic Doppler Current Profiler (Nortek Aquadopp) and optical backscatter sensor (OBS, upper), as well as an Acoustic Doppler Velocimeter (Nortek Vector) and conductivity-temperature-depth sensor (RBR Concerto) and OBS (lower). D) Mastersizer 2000 grain size analyser. E) MX Cubex 50 x-ray source and Cannon Flat Panel x-ray detector used to image sediment cores.

Table 2.1 Oceanographic instruments deployed in this study organized by site and process parameters measured.

	Freshwater				Marine
Parameter	**Site 1**	**Site 2**	**Site 3**	**Site 4**	**Site 5**
Near bed flow velocity	■		■	■	■
Turbidity	■	■	■	■	■
Turbulence	■		■		■
Pressure	■	■	■	■	■
Salinity		■		■	
Temperature		■		■	
Bed movement	■		■		■
Core label	S1C2	S2C1	S3C1	S4C2	S5C1
Instruments deployed	-Aquadopp +OBS	-Vector + OBS -Concerto + OBS	-Aquadopp +OBS	-Vector + OBS -Concerto + OBS	-Aquadopp +OBS

2.2.1 Bathymetry

Five bathymetric surveys, one at each coring and instrument site, were conducted using a vessel-mounted transducer operating at 200 kHz. At each site, data from three to five across-channel transects were collected. Data was subsequently processed using ReefMaster 2.0 and interpolated over the sampling regions to create bathymetry maps to inform the deployment of instruments and collection of vibracores.

2.2.2 Oceanographic instrumentation

At each of the five sites, an instrumented frame was deployed to measure flow conditions near the bed. Each frame included either a downward-looking Acoustic Doppler Current Profiler (ADCP; 2 MHz Nortek Aquadopp) to measure pressure and three components of velocity over a ~40-cm profile (with 25-mm vertical resolution at 8-Hz temporal resolution), or an Acoustic Doppler Velocimeter (ADV; Nortek Vector) which measured velocities at a fixed point at 16 Hz. Sites 2 and 4 also had conductivity-temperature-depth sensors (CTD; RBR Concerto) collecting measurements at 6 Hz. Optical backscatter (OBS) sensors were attached to all instruments to measure turbidity at their respective sampling rates. Seapoint OBS sensors were used with RBR instrumentation while Campbell Scientific OBS3+ were used with Nortek equipment. Nortek instruments were set to record over a 5-minute burst every 15 minutes, while RBR concertos measured continuously. Data processing was conducted using

MATLAB scripts developed by the Coastal Marine Group at the University of Waikato. Nortek data processing consisted of removing atmospheric variations from the pressure record before conversion to depth measurements. While data was of a high quality, a few low quality velocity data (identified by correlations less than 70%) were removed and gaps filled by linear interpolation, and velocities were rotated into east, north, up coordinates. Data were averaged over the burst to provide one data point every 15 minutes. The only processing required for RBR data was the assigning of NaN (not a number) values while gain settings were changing for the turbidity measurements, and these few points were excluded from time averaging. Data was averaged over 15-minute intervals. The dissipation rate of turbulent kinetic energy was calculated per beam from Aquadopp data using the structure function method of Wiles et al. (2006), and with estimates subsequently averaged across the three beams.

OBS sensors were calibrated in the laboratory to provide suspended sediment concentrations from turbidity measurements using bed sediment samples from the field site sieved through a 62.5 μm mesh. The calibration curve was generated in the laboratory by progressively adding sediment to a vessel with pumps to retain the sediment in suspension which also housed the OBS sensors, while taking water samples at set intervals. Water samples were filtered through pre-washed, dried and weighed Whatman glass microfiber filters (GF/C diameter 47 mm), dried for 24 hours at 105 ^{o}C and then re-weighed. This produced calibration curves with r^2 values between 0.91 and 1.00, allowing the turbidity information collected by OBS sensors to be converted to suspended sediment concentrations.

2.2.3 Sediment samples

Surface sediment samples (upper ca. 5 cm) were collected in grids at each site with a Ponar-type grab sampler. These grids consisted of five cross-channel transects spaced from 120 to 500 m along river. Along each transect three to five samples were collected.

The grain size of surface grab samples and core samples were analysed using a Mastersizer 2000 particle size analyser. Prior to being run through the Mastersizer, sediments were sieved though a 3.4 mm mesh, pre-treated with hydrogen peroxide to remove organics, treated with Calgon, and were sonicated to deflocculate clays. Gradistat (Blott & Pye, 2001) was used to statistically analyse grain size data to determine sediment class mean particle diameter using the Folk and Ward (1957) method.

2.2.4 Vibracores

Following instrument retrieval, vibracores were collected from the same mid-locations. A barge with a hiab arm was used to lower the coring tower onto the riverbed prior to activating the vibrating head. The cores were collected in 80 mm diameter aluminium tubing with core catchers at their base and a one-way valve at the top. This process facilitated retrieval of long cores without significant core loss. Upon collection, cores were cut to remove excess tubing, capped to reduce moisture loss, and stood upright to limit percolation of fluids throughout the core. Cores were then stored upright at 6° C in a dark refrigerator. In the laboratory, cores were cut in half with a circular saw and split using a large flat blade. Half of the core was archived while the remaining half was x-rayed, logged, and then sampled for grain size.

2.3 Results and Interpretation

2.3.1 Oceanography

2.3.1.1 Environmental conditions

From the 5th to the 11th of November 2020, precipitation from several storm events increased river levels in the Waihou River catchment and the Ohinemuri River sub-catchment (Figure 2.3). Following the storm, both river levels gradually reduced to approach their baseflow levels by the end of the deployment (November 18, 2020).

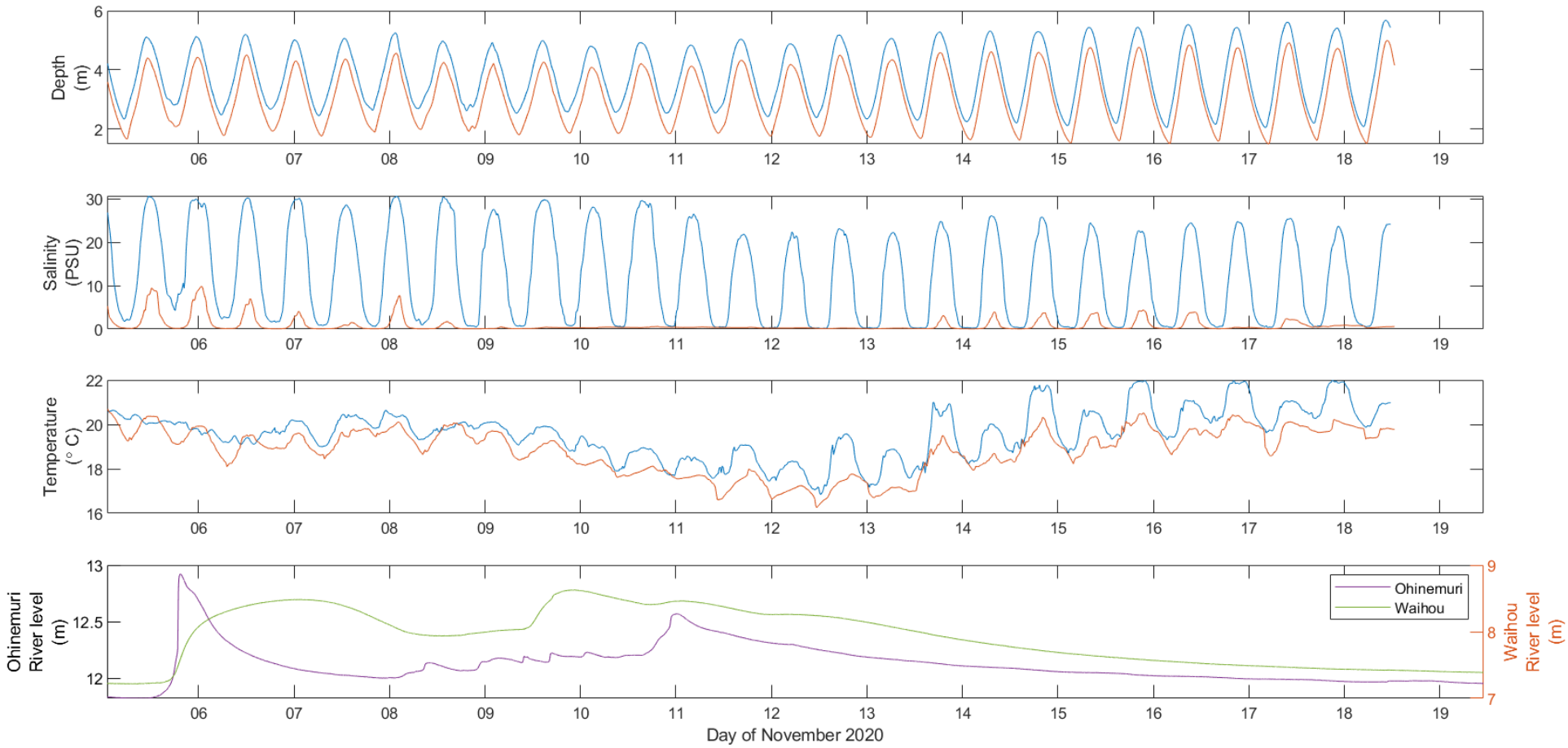

Figure 2.3 Environmental data for Site 2 (yellow) and Site 4 (blue), as well as river level information for the Ohinemuri (purple) and Waihou (green) rivers during the deployment period

2.3.1.2 Process regime - Site 1

Tidal fluctuation in water level at Site 1 ranged from 2.2 m to 3.3 m (above the instrument's pressure sensor which as ~15 cm above the bed) throughout the observation period (Figure 2.4). Current velocities varied between 0 and ca. 0.5 m s^{-1}, reaching their maximum values during the peak of the storm water discharge (Figure 2.4). Currents reversed directions through the tidal cycle, with peak velocities occurring during the last half of the outgoing tide. Flow velocity during the incoming tide was lower, ranging up to 0.3 m s^{-1} (Figure 2.4).

Measurements of suspended sediment concentration (SSC) exceeded their maximum limits of detection (to inferred reliable levels of ca. 3 g L^{-1}) (Figure 2.4). Suspended sediment concentration decreased from high values of >3 g L^{-1} to 0.4–0.5 g L^{-1} as flow velocity approached 0 m s^{-1} as the outgoing tide ended. This pattern was observed during the first three days of deployment, after which time the signal became progressively noisy, and the sensor eventually was buried (10th of November; Figure 2.4).

Backscatter data gave two distinct types of information about the process regime at Site 1 (Figure 2.5). Backscatter intensity contrast was used as a proxy for bed elevation, showing that elevation variations were commonly out of phase with tides. These bed elevation variations fell into two broad categories: 1) short period (within a tidal cycle), low amplitude (up to 0.13 m) variations; and, 2) longer period (several tidal cycles), greater amplitude variations (up to 0.3 m). The short period bed elevations were transient, whereas the longer period changes culminated in a net bed accretion of 0.3 m at Site 1.

Within the water column itself, backscatter intensity was gradational from high to low (upwards through the water column) during times of low river flow velocity (i.e., during the slack tide). These backscatter characteristics occurred at both high and low tide; however, during the high tide the backscatter gradient was more pronounced (producing a zone of low backscatter intensity within the subsurface sediment) (Figure 2.5).

Turbulence dissipation reached maximum values (O(10^{-2}) m^2s^3) during the middle of tidal cycles, while minimum values of O(10^{-6}) m^2s^3 were recorded during periods of slack water throughout the deployment (Figure 2.5). Up until the 13th of November turbulent dissipation rates were greater on outgoing tides (Figure 2.5).

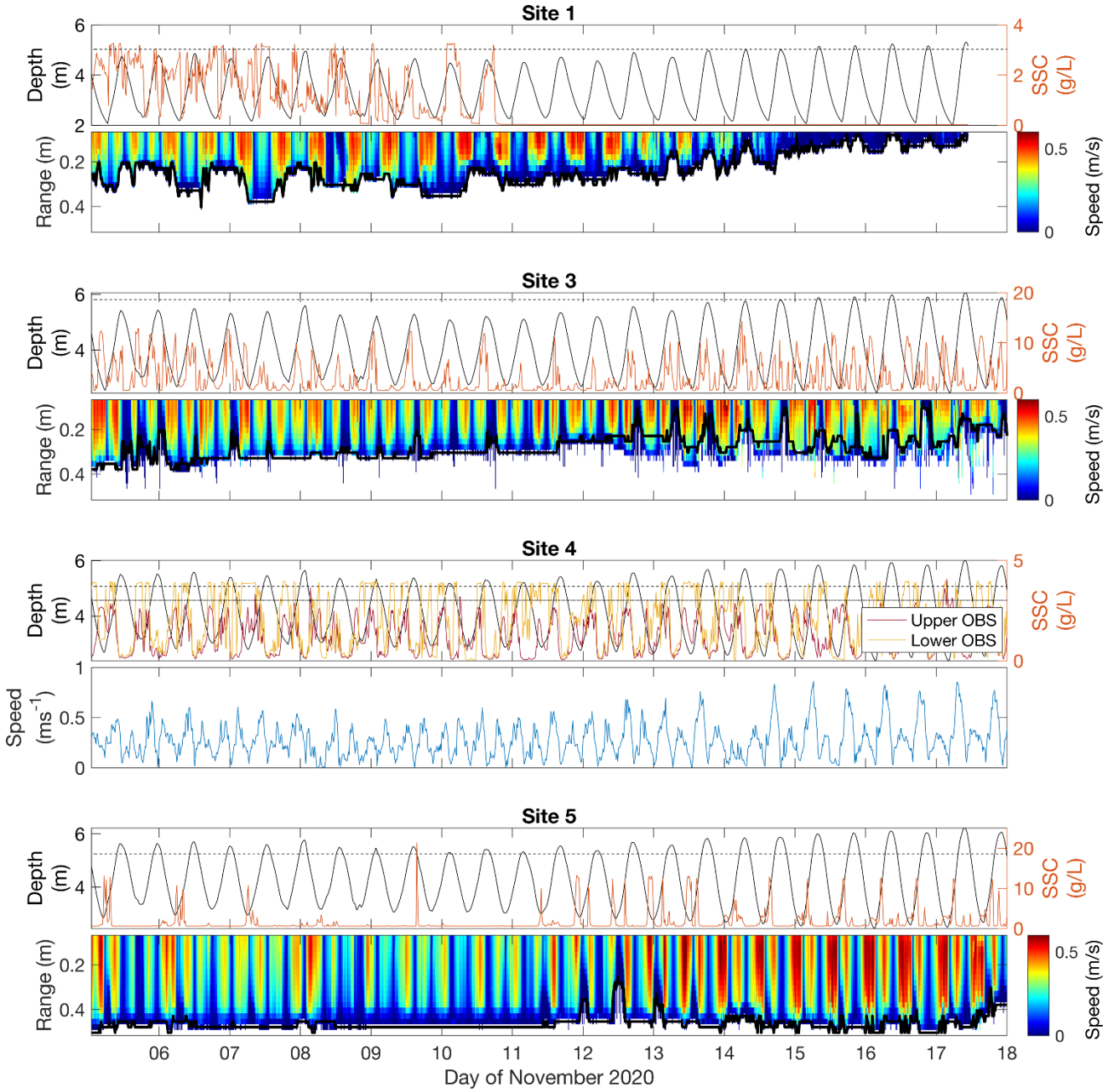

Figure 2.4 Variations in tidal stage, flow velocity, and suspended sediment concentration at Sites 1, 3, 4, and 5. Dashed lines refer to the maximum calibrated SSC values for OBS sensors. Sites 3 and 5 are calibrated up to ~ ca. 18.6 g L^{-1}, Site 1 and the upper OBS sensor at Site 4 (dashed dotted line) are calibrated up to ca. 3 g L^{-1}, and the lower sensor at Site 4 is calibrated up to ca. 3.7 g L^{-1}.

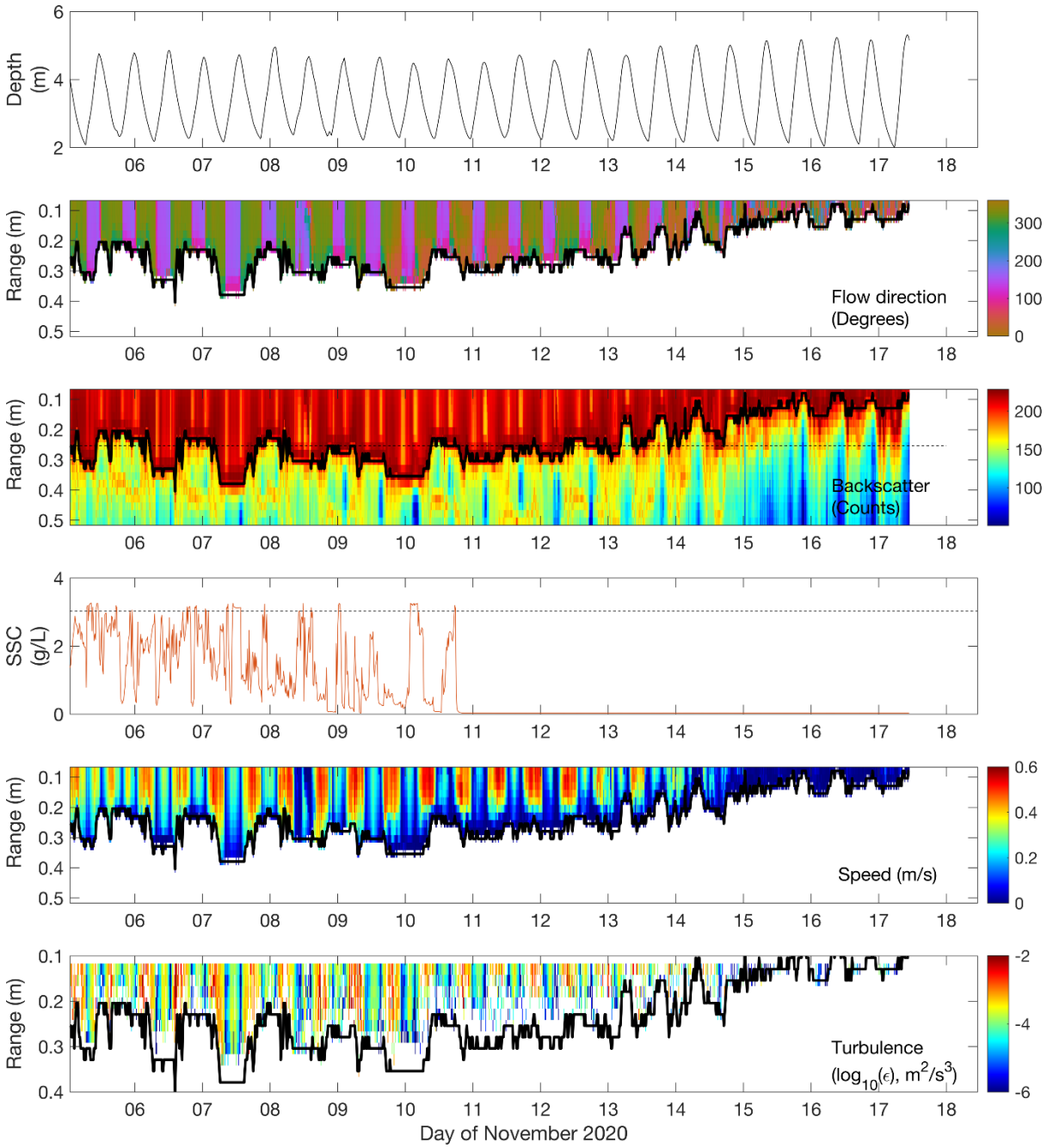

Figure 2.5 Aquadopp ADCP data collected at Site 1. The dashed line on the backscatter subplot represents the theoretical position of the OBS sensor, which was likely buried on the 10th of November 2020. The dashed line on the SSC plot corresponds to the maximum calibrated SSC value for the sensor of ca. 3.7 g L^{-1}. Turbulence is represented by the dissipation rate of turbulent kinetic energy (ε) and is plotted on a log scale (i.e. $\log_{10}(\varepsilon)$).

2.3.1.3 Process Regime - Site 2

Tidal water level fluctuation at Site 2 ranged from 2.23 m to 3.5 m throughout the observation period (Figure 2.3). Water temperature varied from 16.25°C to 20.5° C. Warmer water comes up channel from the Firth of Thames, whereas Waihou River water is cooler (Figure 2.3). The water temperature reflects the mixing of water sources. From the 8th of November water temperature started to decline from 20.5° C to 16.25° C before returning to 20° C by the end of the deployment. The temperature difference between incoming and outgoing tidal stages became more pronounced over the deployment period, with incoming (marine dominated) water being ca. 1° C warmer than the outgoing (river dominated) water by the 13th of November and up to 2.0° C warmer by the end of the deployment (Figure 2.3).

Water salinity varied from <0.1 to 9.8 PSU, achieving maximum values during high tides from the 5th to the 8th of November. From the 9th to the 13th salinity never exceeded 0.5 PSU. From the 13th to the 18th of November, peak water salinity during high tide was slightly lower, ranging up to 4.4 PSU, while during low tides salinity decreased to < 0.1 PSU (Figure 2.3).

2.3.1.4 Process Regime - Site 3

Within the observation period, tidal fluctuation in water level at Site 3 ranged from 2.33 m to 3.55 m (Figure 2.4 and Figure 2.6). Current velocities varied between 0 and ca. 0.6 m s^{-1}, reaching their maximum between the 12th and 15th of November (Figure 2.4). Currents reversed directions through the tidal cycle, with peak velocities measured on both incoming and outgoing tides. Generally, the outgoing flow speeds were slightly faster than those on the incoming tide (Figure 2.4).

The peaks in turbidity can be correlated with high flow velocities at the bed (most commonly on the incoming tide) (Figure 2.4). Suspended sediment concentration decreased from the high values of up to 14 g L^{-1} to 0.5 g L^{-1} as flow velocity approached 0 m s^{-1} at the end of incoming tides. From the 9th to the 13th there were single clean peaks on incoming tides, whereas outside of that period there were multiple peaks, with a notable peak developing at the end of the outgoing tide, terminating on slack water (Figure 2.4).

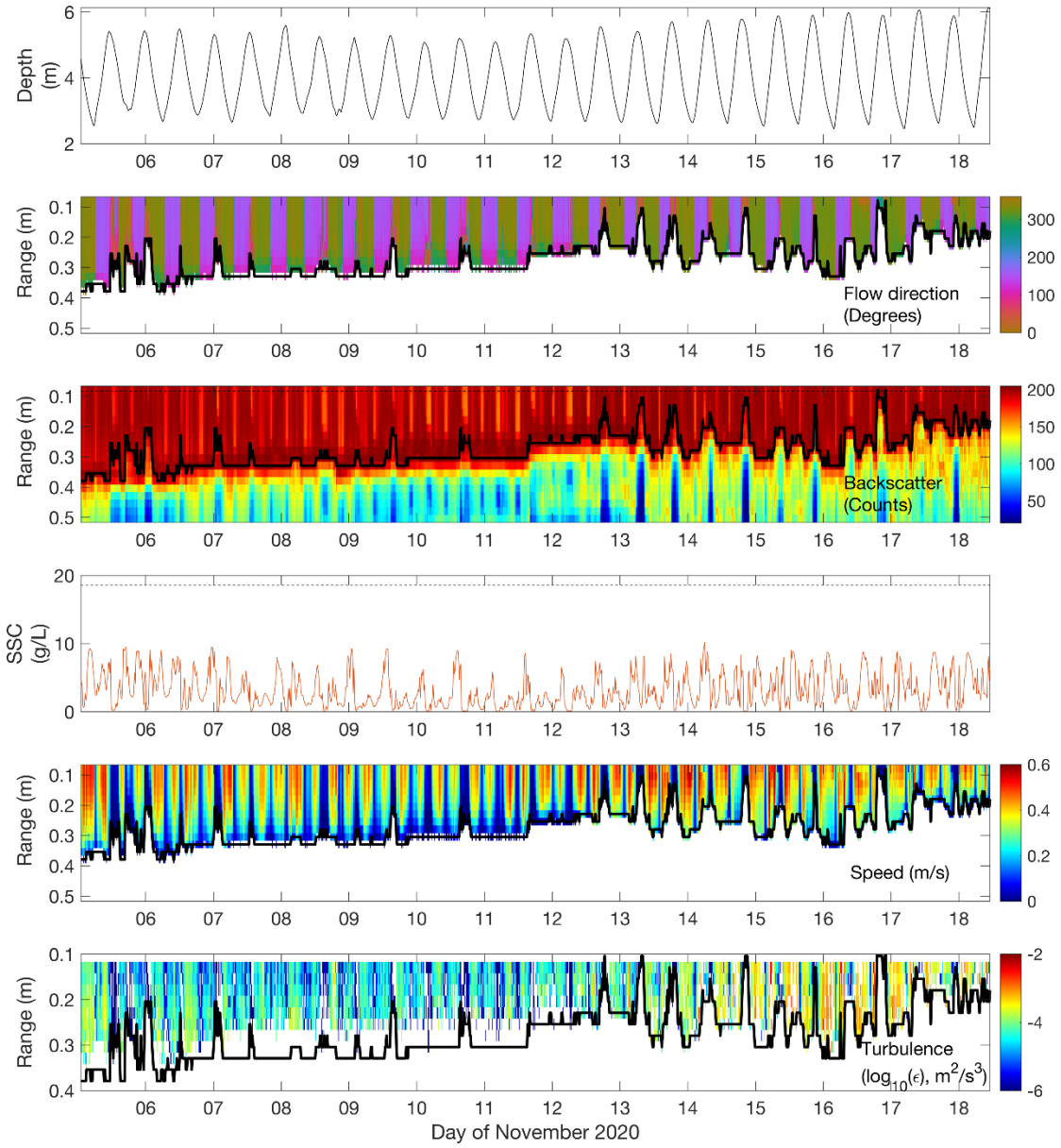

Figure 2.6 Aquadopp data collected at site 3. Dashed line on backscatter subplot represents the theoretical position of the OBS sensor. The dashed line on the SSC plot corresponds to the maximum calibrated SSC value for the sensor of ~18.6 g/L. Turbulence is represented by the dissipation rate of turbulent kinetic energy (ε) and is plotted on a log scale (i.e. $\log_{10}(\varepsilon)$).

Similar to Site 1, bed elevation as measured by backscatter intensity displayed both short period (within a tidal cycle), low amplitude (>0.2 m) variations that were commonly in phase with tidal movements, as well as longer period, greater amplitude variations (spanning multiple tidal cycles) (Figure 2.6). The culmination of the long period variation was a net bed accretion of 0.2 m. The short period variations in bed elevation were commonly associated with decreases in backscatter intensity within the water column while lower backscatter intensities (below ~100 counts) were observed within the subsurface sediment. These features occurred at both high tide and low tide and were associated with a decrease in the water column backscatter intensity. The high tide features were more pronounced and were also associated with a decrease in the backscatter intensity to below ~100 counts in the subsurface sediment (Figure 2.6).

Turbulence dissipation reached maximum values of $O(10^{-2})$ m^2s^3 during the middle of tidal cycles, while minimum values of as low as $O(10^{-6})$ m^2s^3 were recorded during periods of slack water throughout the deployment (Figure 2.6). From the start of the deployment until mid-way through the 11th of November the turbulence dissipation was greater on the outgoing tide than the incoming. After the 11th, higher turbulence dissipation rates were measured on the incoming tide (Figure 2.6).

2.3.1.5 Process Regime - Site 4

Tidal fluctuation in water level at Site 4 ranged from 2.3 m to 3.6 m across the deployment period (Figure 2.4). Water temperature varied from 16.85°C to 22° C (Figure 2.3). Warmer water was derived from the Firth of Thames, whereas Waihou River water was cooler. From the 8th of November water temperature started to decline from 20.1° C to 16.85° C before rising to 21.95° C by the end of the deployment. The temperature difference between incoming and outgoing tidal stages became more pronounced over the deployment period, with incoming (marine dominated) water being ~1° C warmer than the outgoing (river dominated) water by the 13th and up to 2.5° C warmer by the end of the deployment (Figure 2.3).

Water salinity varied from 0.5 to 30.5 PSU with maximum values recorded during high tides (Figure 2.3). During low tides from the 5th to 11th water salinity decreased to 0.5 to 2 PSU. From the 12th to the 18th of November, peak water salinity during high tide was slightly lower

ranging up to 24 PSU, while during low tides salinity decreased to 0.5 PSU. Minimum peak salinity was recorded on the 11th of November (Figure 2.3).

Current velocities varied between 0 and ~0.8 ms^{-1}, reaching their maximum values between the 13th and 18th of November (Figure 2.4). Currents reversed directions through the tidal cycle, with peak velocities occurring on incoming tides. Flow velocities during the outgoing tides were lower, ranging up to 0.4 m s^{-1} (Figure 2.4). Observations of SSC exceed maximum measurable values for both sensors, to inferred reliable levels of ca. 3.7 g/L at the lower senor and to 3.0 g/L at the upper sensor (Figure 2.4). Suspended sediment concentration commonly decreased from the high values (of >3.7 g/L for the upper sensor and ~2.5 g/L for the lower sensor) to < 0.1 g/L as flow velocity approached zero resulting in a bimodal type peak across slack water. A lower bound for the vertical SSC gradient commonly measured during the deployment is 0.0625g/L/cm (Figure 2.4).

2.3.1.6 Process Regime - Site 5

Within the observation period, tidal fluctuation in water level at Site 5 ranged from 2.3 m (10th November) to 3.7 m (17th November) (Figure 2.4).

Current velocities varied between 0 and ~0.6 m s^{-1}, reaching their maximum values between the 12th and 15th of November on both outgoing and incoming tides (Figure 2.4). Currents reversed directions through the tidal cycle; incoming current velocities were generally greater than outgoing velocities prior to the 13th; however, the opposite was true after the 13th (Figure 2.4).

Observations of SSC maxed out to inferred reliable levels of ca. 18.6 g/L on the 9th just after hightide, however more commonly SSC would peak up to ~13 g/L either side of low tide (Figure 2.4); suspended sediment concentration decreased from these high values to ~0.6 g/L as flow velocity approached zero (Figure 2.4).

The position of the bed trace was relatively stable at site 5 for much of the deployment period; movement of the bed trace was characterised by both short period (within a tidal cycle), (amplitude >0.21 m) variations that were commonly in phase with tidal movements, as well as longer period variations (spanning multiple tidal cycles) (Figure 2.7). The culmination of the long period variation was a net bed accretion of 0.05 m. Decreases in water column backscatter intensity occurred at both high and low tide, however the short period variations in bed elevation only occurred at low tide (Figure 2.7).

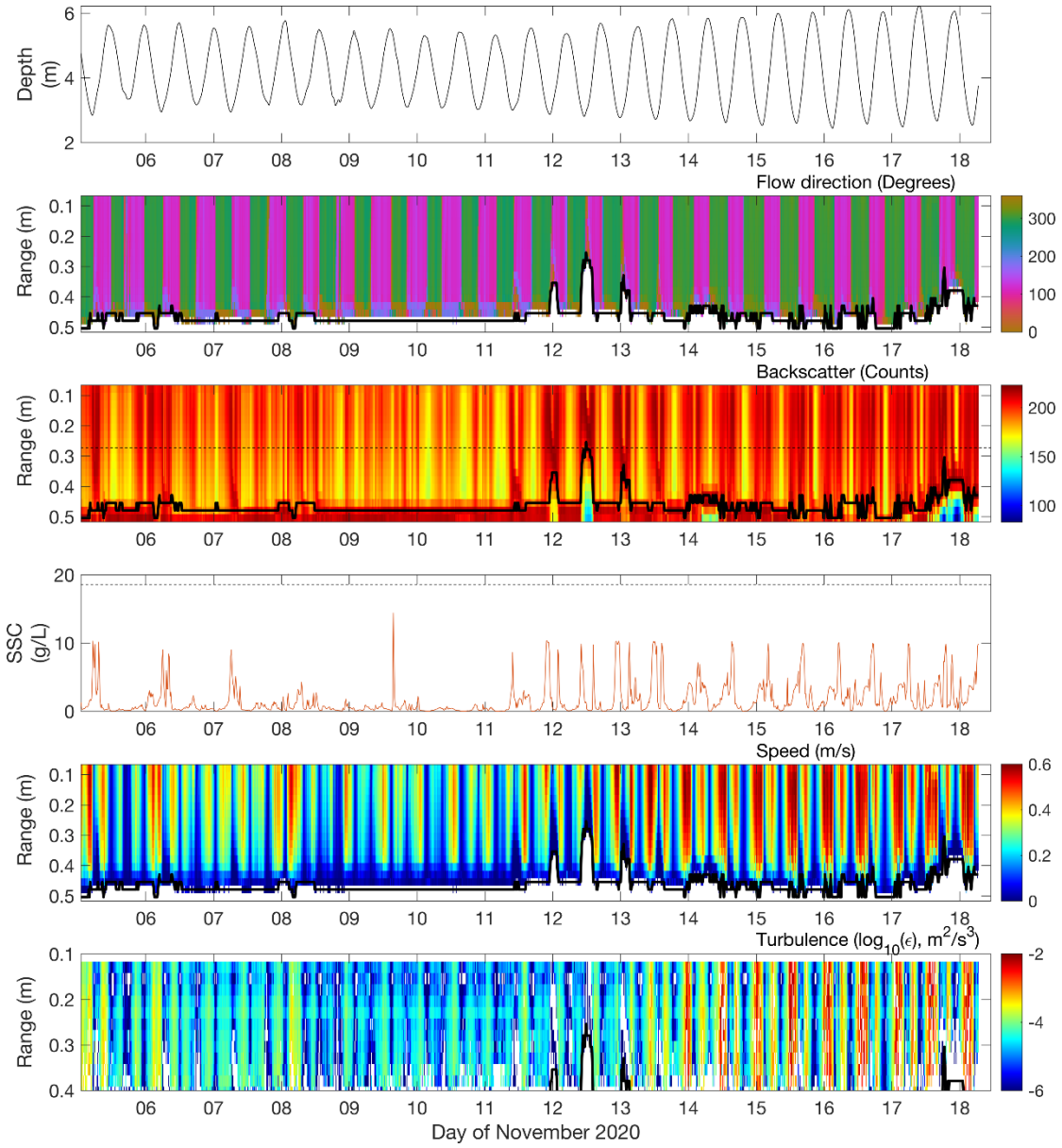

Figure 2.7 Aquadopp data collected at site 5. Dashed line on backscatter subplot represents the theoretical position of the OBS sensor. The dashed line on the SSC plot corresponds to the maximum calibrated SSC value for the sensor of ~18.6 g/L. Turbulence is represented by the dissipation rate of turbulent kinetic energy (ε) and is plotted on a log scale (i.e. $\log_{10}(\varepsilon)$).

Turbulence dissipation reached maximum values (of O(10^{-2}) m^2s^3 on the 15th) during mid-outgoing tide, while minimum values of O(10^{-6}) m^2s^3 were recorded during periods of slack water throughout the deployment (Figure 2.7). From the start of the deployment until mid-way through the 13th the turbulence dissipation was greater on the incoming tide than the outgoing tide; after the 13th, greater turbulence dissipation rates were measured on the outgoing tides (Figure 2.7).

2.3.2 Bathymetry and Sedimentology

The cored sedimentary successions at the five locations revealed that there are seven recurring sedimentary packages (i.e., facies). Examples of each facies are presented in Figure 2.8, while the distribution of facies within the cores is displayed in Figure 2.9. Table 2.2 summarizes the distinguishing characteristics of each unit. These sedimentary facies are interpreted in the context of the growing body of literature on the FMTZ, and especially the recognition of dynamically deposited muds (Baas et al., 2009; Dalrymple & Choi, 2007; Mackay & Dalrymple, 2011; Macquaker et al., 2010; McCave, 1970; Mulder et al., 2003).

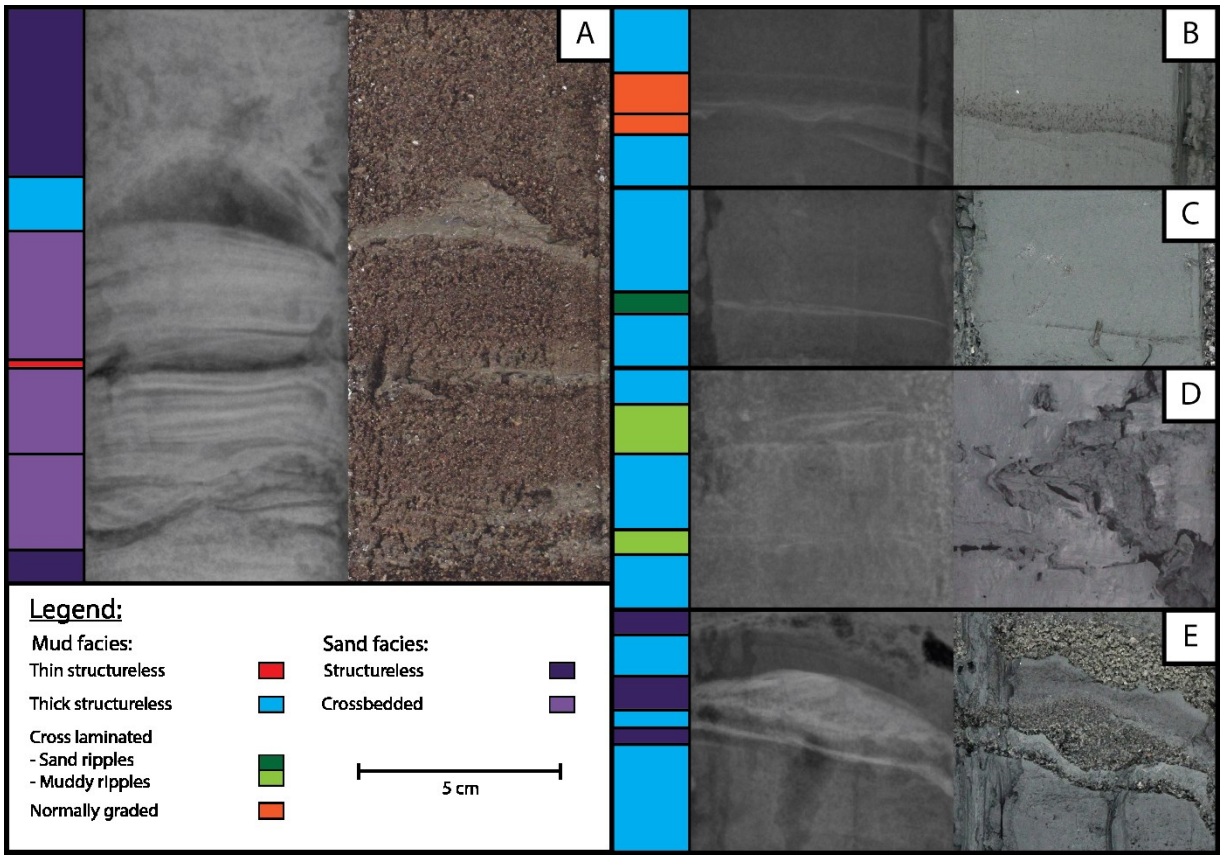

Figure 2.8 Facies present in the vibracores collected from the FMTZ of the Waihou River FMTZ. Each example shows an x-radiograph next to its corresponding core photograph.

Table 2.2 Summary table showing the features of the seven facies identified in the Waihou River FMTZ.

Facies	Thickness	n	Contacts	Grainsize	Depositional Process
Unstratified facies					
Thin structureless mud (Facies A)	<2.5 mm	3	Sharp basal; sharp or gradational upper	Homogeneous fine to coarse silt	Gravitational settling
Thick structureless mud (Facies B)	3-100 mm	85	Sharp basal; sharp, loading structures or gradational upper	Homogeneous fine to coarse silt	Quasi-laminar plug or unstable plug flow
Normally graded mud (Facies C)	5-20 mm	9	Sharp basal; sharp or gradational upper	Heterogeneous mixture of silt and very-fine sand	Waning currents
Structureless sand (Facies D)	2.5-215 mm	55	Sharp or gradational basal; sharp or gradational upper	Silty fine sand to fine gravely coarse sand	Rapidly decelerating flow
Stratified facies					
Cross-laminated mud - muddy ripples (Facies E1)	2-15 mm	28	Sharp basal; sharp or gradational upper	Fine to coarse silt	Transitional-turbulent, or transitional-plug flow
Cross-laminated mud - Sandy laminations (Facies E2)	3-15 mm	21	Sharp basal; sharp or gradational upper	Fine silt to very-fine sand	Transitional-turbulent, or transitional-plug flow
Cross-bedded sand (Facies F)	17-145 mm	43	Sharp or gradational basal; sharp or gradational upper	Silty medium sand to very-fine gravely coarse sand	Turbulent flow

Facies A constitutes thin structureless mud (<2.5 mm), interpreted as the depositional product of gravitational settling from the water column at slack tide (Mackay & Dalrymple, 2011; McCave, 1970) (Figure 2.8A). Facies B comprises structureless mud thicker than 2.5 mm (Figure 2.8A-E). These beds are interpreted as fluid mud layers that have frozen to the bed under unstable-plug flow (Baas et al., 2009; Mackay & Dalrymple, 2011). Facies C is composed of normally graded mud beds (Figure 2.8B), which are interpreted to represent the unidirectional waning currents (e.g. sediment gravity flows or the last stages of muddy hyperpycnal currents) (Macquaker et al., 2010; Mulder et al., 2003). Facies D constitutes structureless sand beds (Figure 2.8A) that are inferred to be the product of rapid deceleration of sediment laden flows (Shanmugam, 1997). Facies E (subdivided into E1 and E2) is composed of cross-laminated mud beds, interpreted to represent traction transport of sediment under turbulent, transitional-turbulent, or transitional plug flow (Baas et al., 2009; Mackay & Dalrymple, 2011). Facies E1 are muddy ripples (Figure 2.8D), while Facies E2 are sandy grain size gradational ripples Figure 2.8. Facies F is cross bedded sand (Figure 2.8C), and is interpreted to form under turbulent flow and is the depositional expression of ripples and dunes that migrate over the bed (Dalrymple & Choi, 2007).

2.3.2.1 Site 1

The Waihou River at Site 1 was 220 m wide (measured across-channel and intersecting the core), with a maximum depth of 6.5 m along the eastern cut bank (Figure 2.9). The proportion of mud within surface sediments at Site 1 was greatest along the eastern bank and into the base of the channel (up to 98.46% mud), while the wide point bar on the western bank was sand dominated (as low as 3.45% mud). The mean proportion of mud within the surface samples collected at site 1 was 44.65%.

The core collected from Site 1 was 276 cm long. The majority of the core (below 27cm) is rhizoturbated mud (i.e., rooted to the point of destroying most primary physical sedimentary structures), although contains 3 to 8 mm thick beds of Facies E1 (Figure 2.10). The upper portion of the core is sand dominated and features both Facies D (100 mm thick) and Facies F (34 to 50 mm thick). Overall the core displays a coarsening upwards trend.

2.3.2.2 Site 2

The Waihou River channel is 352 m wide at Site 2, with a maximum depth of 5 m along the southern bank (Figure 2.9). The proportion of mud within surface sediments at Site 2 was greatest along channel margins and atop the mid-channel bar (up to 90.28% mud), while the base of the channel was sand dominated (as low as 4.79% mud). The mean proportion of mud within the surface samples collected at site 2 was 47.87%.

The core collected from Site 2 was 128 cm thick. The base of the core is sand dominated, with 1 to 3 cm thick beds of Facies D and Facies F interspersed with ca. 1cm thick beds of Facies B. These deposits grade upward into thicker beds of Facies B and thinner sand beds up to approximately 100 cm depth. Above this depth, the core is completely mud-dominated. From 100 cm to 65 cm the core is composed of thick beds (up to 100 mm) of Facies B interbedded with thin (< 1.5 cm) beds of Facies E1 and E2. Above 65cm, thick beds of Facies D (up to 55 mm) and F (up to 195 mm) make up the majority of the core, only interrupted by a few beds of Facies A and Facies B. Overall the core represents a coarsening upwards package of sediment.

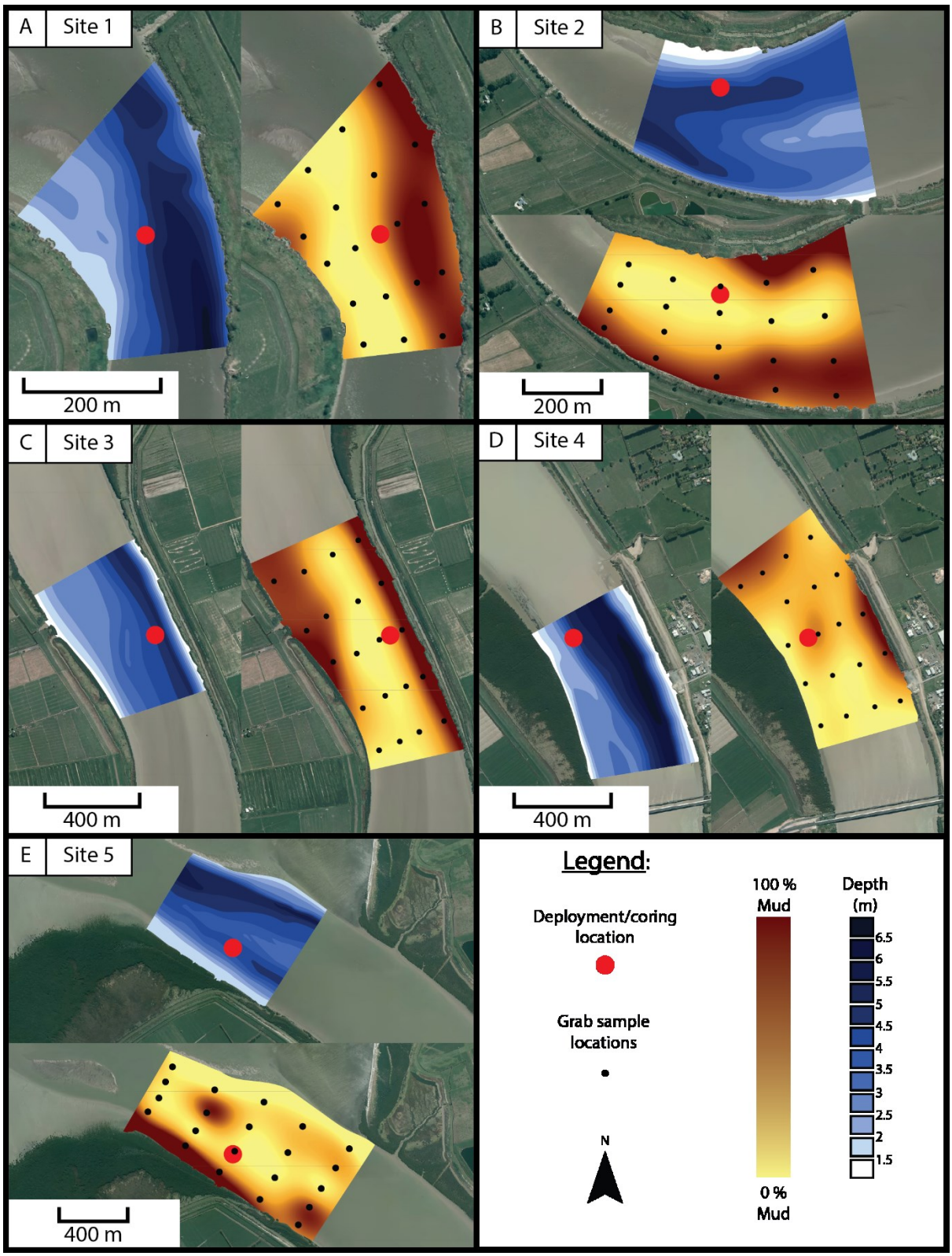

Figure 2.9 Maps showing the bathymetry and proportion of mud at each of the five sites along the FMTZ of the Waihou River.

2.3.2.3 Site 3

The width of the river channel at Site 3 is 420 m, with a maximum depth of 5 m along the eastern bank.

The proportion of mud within surface sediments at Site 3 was greatest along channel margins and over the broad plain against the western bank (up to 96.42% mud), while the base of the channel was sand dominated (as low as 4.38% mud). The mean proportion of mud within the surface samples collected at Site 3 was 50.48%.

The core collected from Site 3 was 203 cm long. The majority of the core (below ca. 40 cm) was mud dominated and comprises of a mixture of thin (<5 mm) interbeds of Facies B and Facies E1 or Facies E2, interbeds (10 to 20 mm thick) of Facies C and Facies D, and rarely beds of facies A or Facies F. The upper portion of the core (above 40 cm) is composed of equal proportions of Facies D and Facies F (20 to 70 mm thick beds) with a singular bed of Facies B.

2.3.2.4 Site 4

The width of the Waihou River channel at Site 4 is 432 m, with a maximum depth of 6.5 m along the eastern bank. The proportion of mud within surface sediments at Site 4 was greatest along the eastern channel margin, and to a lesser extent, down into the base of the channel in places (up to 86.44% mud). The majority of the channel base was sand dominated (as low as 6.79% mud). The mean proportion of mud within the surface samples collected at Site 4 was 36.49%.

The vibracore from Site 4 was 109 cm long. The base of the core was mud dominated and was composed of thick (6 to 60 mm) beds of Facies B interbedded with thin (3 to 20 mm) beds of Facies E1. Above 75 cm core depth, sand beds (Facies D and F) are interspersed within the beds of Facies B, while Facies E2 is more common than Facies E1. Above 40 cm core depth is characterized by thick (widths of up to 215 mm) beds of Facies D. Overall the core displays a coarsening upwards package of sediment.

2.3.2.5 Site 5

At Site 5 the Waihou River is 650 m wide and has a maximum depth of 5.5 m, although the deployment site was not positioned within the main thalweg, rather in smaller side channel which only reaches 4.5 m deep (Figure 2.9).

The proportion of mud within surface sediments at Site 5 was greatest along the south-western channel margin (up to 98.1% mud); there was also mud deposited locally within the base of the channel, but most of the channel base was sand dominated (as low as 3.85% mud). The mean proportion of mud within the surface samples collected at site 5 was 34.93%.

The core collected from Site 5 was 92 cm long and was sand dominated. The core comprises predominantly thick beds of Facies D (up to 140 mm) with a few beds of Facies F (up to 50 mm). There were also two beds of facies B in the upper 25 cm of core. The sediment package slightly coarsens upwards.

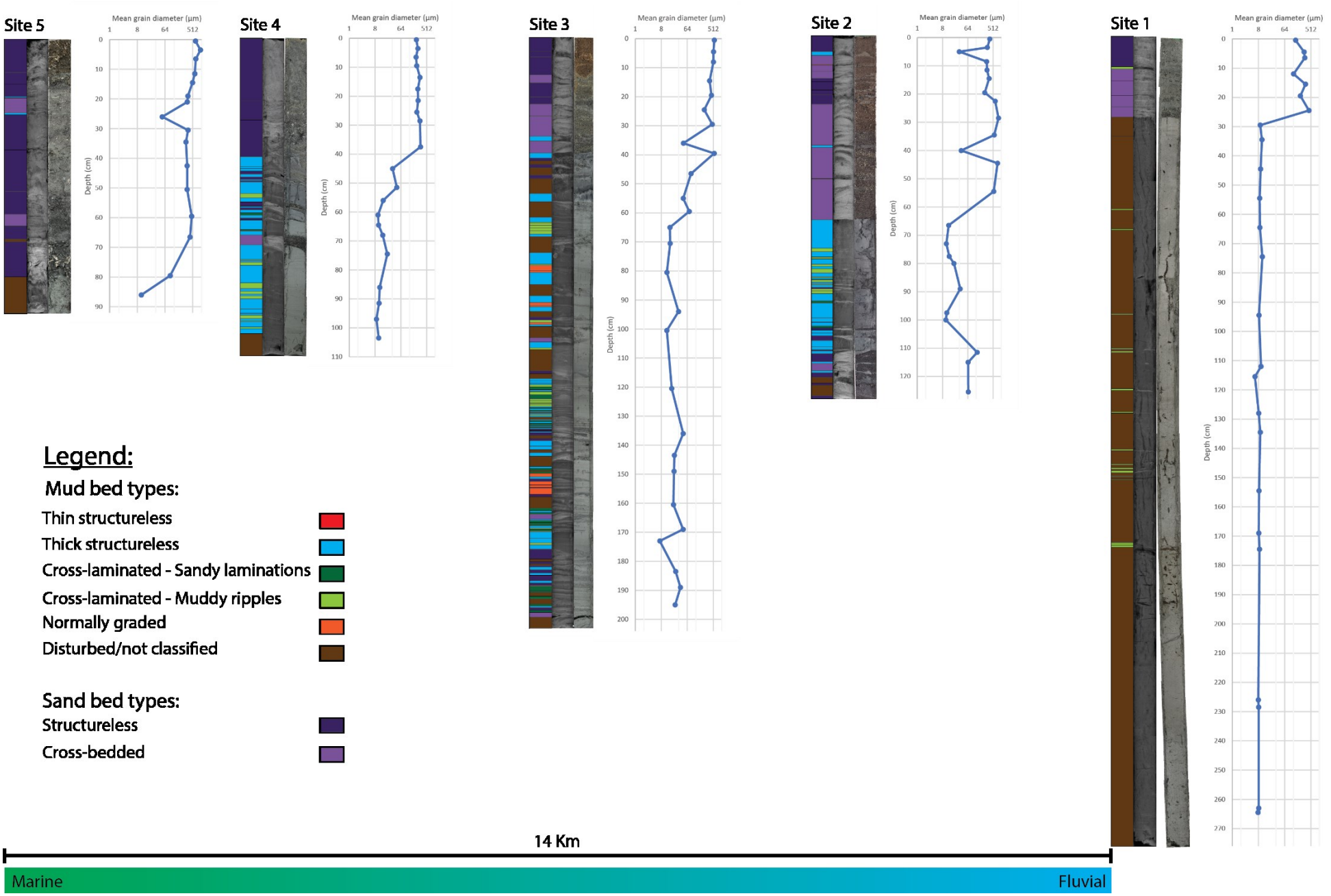
Site 5
Site 4
Site 3
Site 2
Site 1
Mean grain diameter (µm)
Depth (cm)
Legend:
Mud bed types:
Thin structureless
Thick structureless
Cross-laminated - Sandy laminations
Cross-laminated - Muddy ripples
Normally graded
Disturbed/not classified
Sand bed types:
Structureless
Cross-bedded
14 Km
Marine
Fluvial

Figure 2.10: Vibracores collected across the FMTZ of the Waihou River. From left to right for each core displays the facies interpreted, an x-radiograph, a core photograph, and the mean grain size of. Spacing between cores are to scale, but they are not hung on a datum.

2.4 Discussion

The purpose of this study is to construct process-response linkages for sedimentary successions that accumulate across the FMTZ to improve existing depositional models, with emphasis on the distribution and characteristics of mud types. To this end, in this section I first describe the landward to seaward trends for both physical sedimentary processes and sediment characteristics separately, and then construct linkages between the two datasets.

2.4.1 Broad Trends in Hydrodynamic Processes

Salinity variation throughout the lower Waihou River is ultimately controlled by the incursion of marine water into channels driven by tidal forcing and opposed by river discharge. With high tide, regardless of river discharge, the seaward end of the lower Waihou River (i.e., at least to Site 4) experiences polyhaline conditions (Figure 2.3). By contrast, the landward portion of the lower Waihou River (i.e., Site 2), is periodically subjected to mesohaline conditions during spring tide and / or low river discharge. Using a 2.85 PSU / km gradient in salinity reduction, I estimate that the maximum landward limit of marine water incursion occurs at approximately 350 m seaward of Site 1. Therefore, the deployment sites from 1 to 5 appear to be located in positions that capture the entire brackish-water zone within the lower Waihou River.

Generally, peak flow speeds increase from landward to seaward across the study area. However, the peak flow speeds taper off at the most seaward site (Figure 2.11). Peak flow speeds occur during ebbing tides at the landward end of the study area, and shift to flood dominance near the mouth of the Waihou River. This change reflects the fact that the landward portion of the study area is river-dominated and the seaward end is marine-dominated. This relationship also suggests that a bedload convergence zone (BLC), where seaward transported sediment from the river meets landward transported sediment from the ocean, occurs in close proximity to Site 2 (Figure 2.11).

At the most seaward position within the study area, currents within an ebb-dominant side channel were measured. This was a product of not being able to place the site with the main channel (as it would be a navigational hazard), and thus it was positioned on the opposite side

of a mid-channel bar to the main channel. The peak flow velocities at Site 5 were measured on outgoing tides while peak flows at Site 4 were measured on incoming tides. This result suggests that the flow may be bifurcating, setting up an ebb-dominant side channel, while the main channel may still remain flood dominant (as at Site 4). This split would explain the discrepancy in peak velocity timing and magnitude between Site 5 and Site 4.

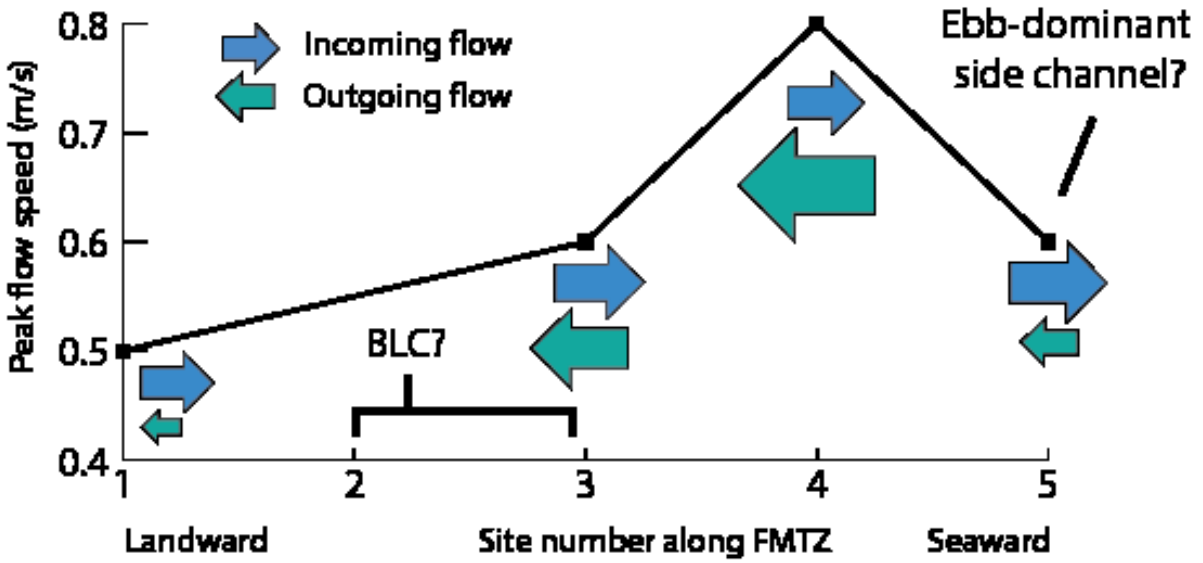

Figure 2.11 Peak flow speeds along the Waihou River FMTZ and the relative strength of tides.

The periodicity and amplitude of bed elevation changes, as inferred from backscatter intensity contrasts, varies across the FMTZ. Landward, bed elevation changes over long periods resulted in considerable net bed sediment accretion (which ultimately buried the sensors). In the middle of the study area, and at the more seaward sites, long period changes in bed elevation were less pronounced but there were many short period, low amplitude changes. These short period shifts were consistently in-phase with the tides. The variations in bed elevation were (and as a standalone phenomenon at Site 1) matched by decreases in backscatter intensity within the water column. These backscatter intensity changes are inferred to be the rapid settling of sediment from the water column. Correspondingly, the short period changes in bed elevation are interpreted to be the flocculation of suspended sediment and accumulation of these floccules into fluid mud layers along the bed. Further support for the interpretation of fluid muds is the decrease in flow speed, decrease in water column backscatter, and decrease in SSC at the OBS sensor which all occur in unison with these short period bed elevation changes (Figure 2.12). Importantly, OBS sensors were positioned 0.14-0.33 m above the bed, and therefore, fluid mud accumulating on the bed

would not be thick enough to be detected by the sensor (i.e., the OBS signal reflects 'clearing' of the water column). Fluid muds are interpreted to accumulate at high tide at the landward end of the study area and at low tide at the seaward end. This relationship reflects the location of the mixing front (i.e., the turbidity maximum zone; (c.f. La Croix and Dashtgard (2014)).

Suspended sediment concentrations were varied over the tidal cycle, and measurements at some sites were limited by the maximum resolvable concentration of some of the instruments. However, for the OBS sensors with large ranges, turbidity values corresponding to very large SSCs were observed (up to 18 g/L), with fluid mud regularly occurring at slack tides (based on backscatter data). It is postulated that the clearing of the water column means that SSC values well in execs of the measured maximums are occurring near the bed as fluid muds.

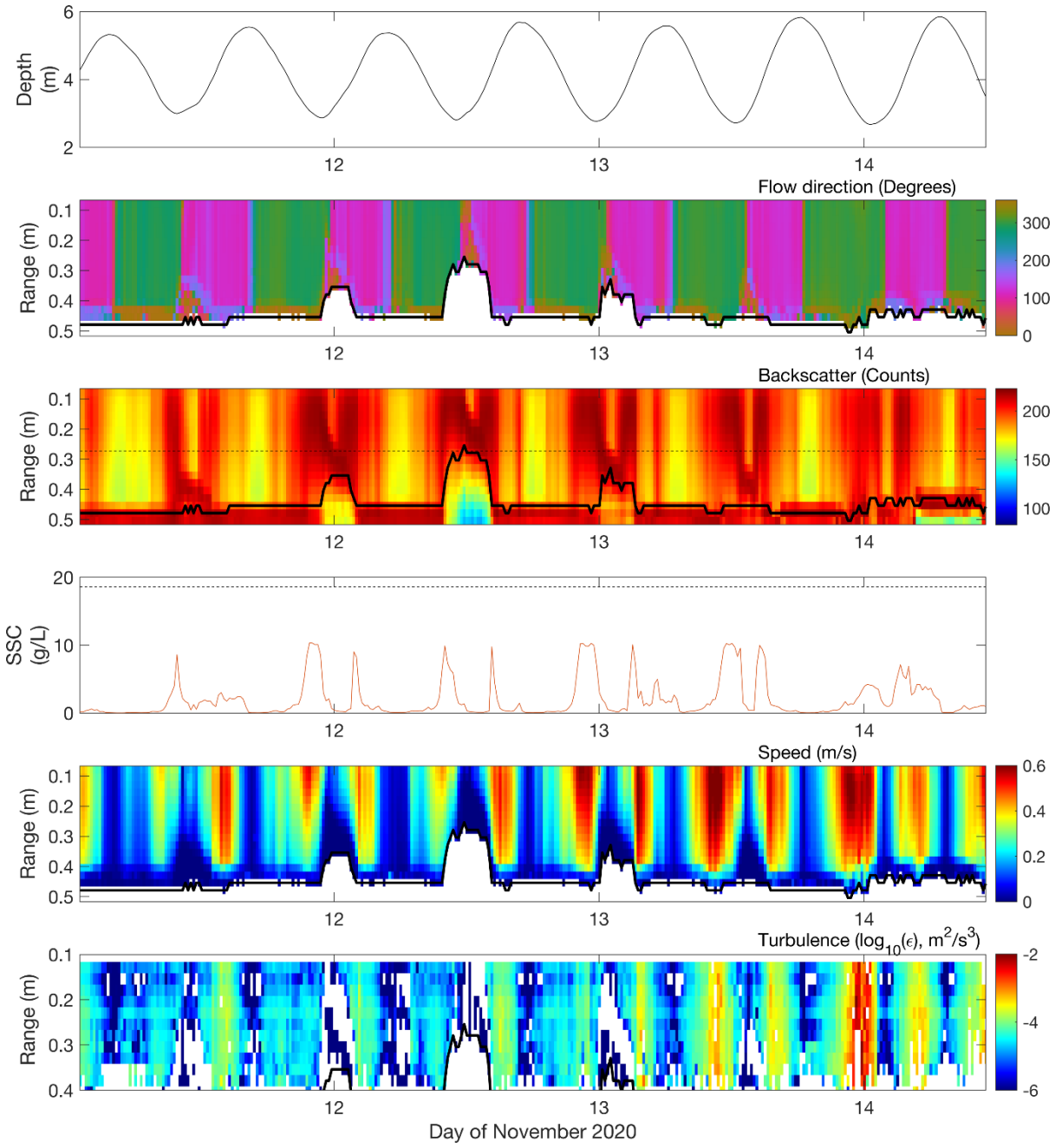

Figure 2.12 Example of what are interpreted to be fluid muds accumulating and eroding at site 5 within the Waihou River FMTZ.

2.4.2 Broad Trends in Sedimentology

Along the entire FMTZ, mud deposition is for the most part localized along channel margins and atop mid channel bars. However, mud accumulates at the base of channels as well (Figure 2.9). The average mud content of surface sediments shows the locus of mud deposition is situated near Site 3 and the highest proportion of sand occurs at the marine end of the lower Waihou River (Figure 2.13). In other words, the turbidity maximum zone occurs in the vicinity of Site 3, right in the middle of the study area.

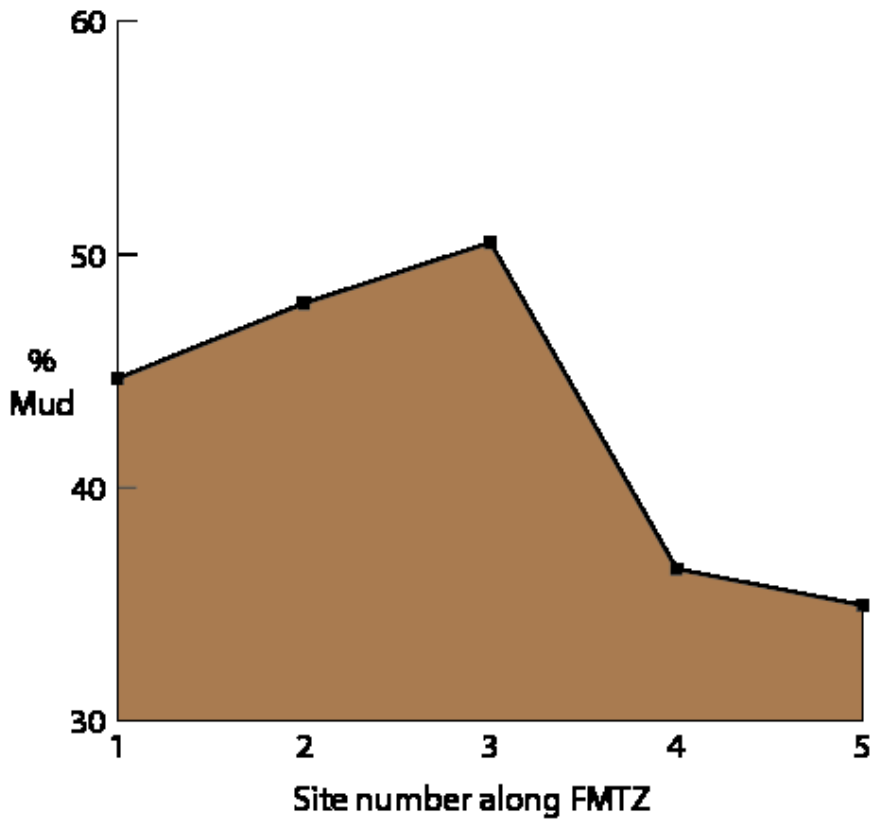

Figure 2.13 Average proportion of mud within surface samples collected at each site throughout the Waihou River FMTZ. Site 1 is the most landward site and site 5 is the most seaward.

From landward to seaward through the lower Waihou River there is a systematic change in the amount and types of mud facies (Figure 2.14). Overall, the greatest diversity of mud facies occurs near the locus of mud deposition at Site 3, which records all five mud facies types in its stratigraphic record. Cores from the most landward and seaward locations differ in that they only display one mud facies type (Facies E1 and Facies B, respectively). Cores collected from intermediate positions (i.e., Sites 2 and 4) have very similar mud facies assemblages present in their stratigraphy. However, Site 4, which is located more seaward than Site 2, contains Facies A, whereas Site 2 does not. By contrast to the mud facies, all cores display similar sand facies (Facies D and Facies F), indicating that sand facies types are a poor predictor of depositional position.

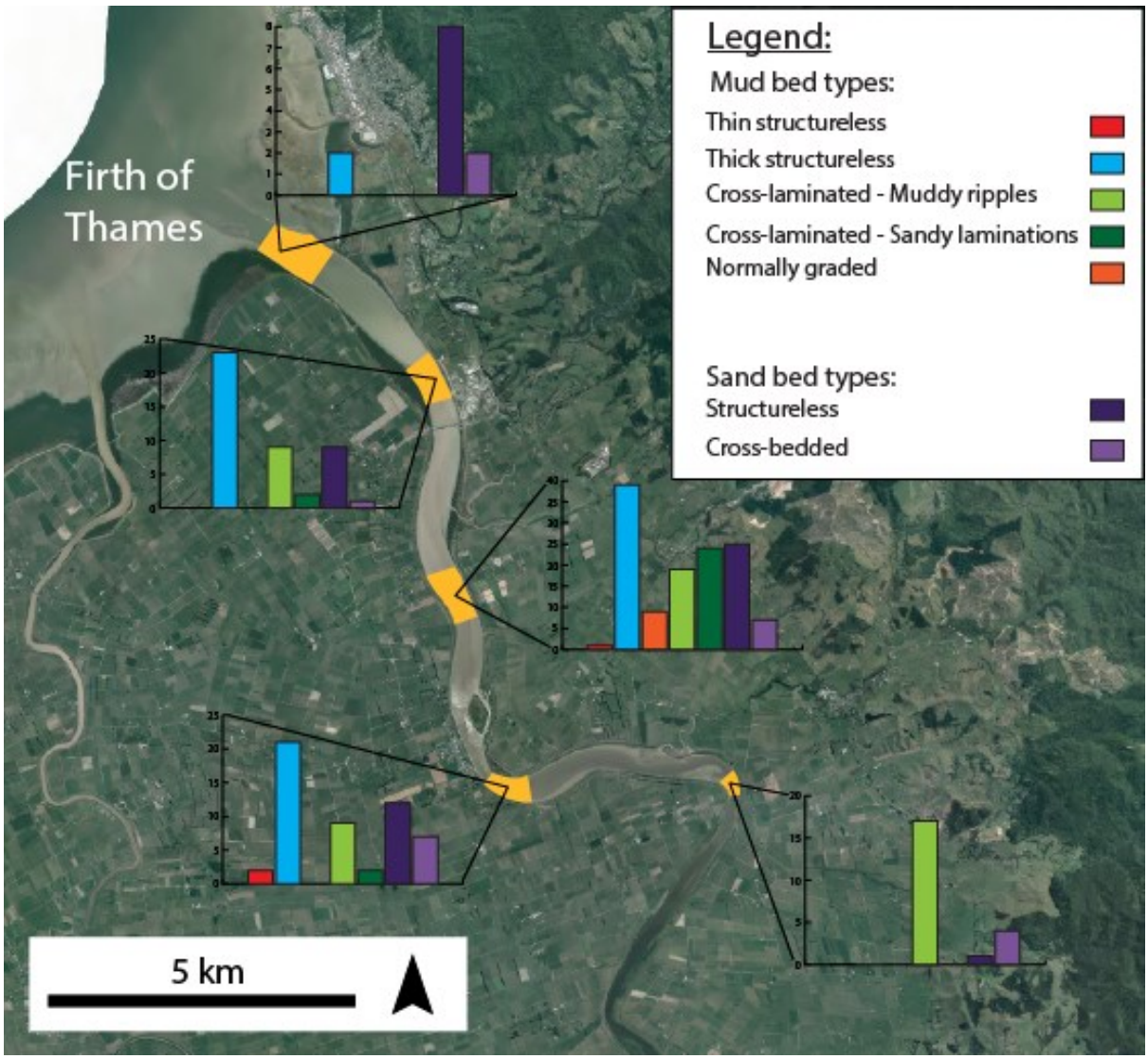

Figure 2.14 Facies distribution across the Waihou River FMTZ.

2.4.3 Process-response linkages

Net accumulation of mud within the lower Waihou River, which reaches its maximum in the vicinity of Site 3, is due to a combination of depositional and preservation factors. The landward limit of mud deposition is controlled by the maximum extent of marine water intrusion into the channel. Site 1 is situated beyond the landward extent of the mixing front, and fluid muds do not develop within channels, although mud is deposited on channel bars. By contrast, at the seaward end of the study area, near Site 5, mixing of marine and freshwater regularly occurs, and fluid muds commonly develop at the bed. However, the preservation potential of mud deposits is low due to higher flow speeds reworking the bed; as a result, the seaward end of the system is sand-dominated; Dalrymple et al. (2003) used a similar theory to justify the absence of fluid muds in parts of distributary channels of the Fly

River delta. Peak mud deposition in the Waihou system occurs in the middle of the turbidity maximum zone, where the process regime and preservational characteristics of mud facilitates its long-term accumulation. Similar overall trends in mud proportions along the FMTZ's of the Fraser River (La Croix & Dashtgard, 2014) and Mekong River (Gugliotta et al., 2017) delta systems have been identified. However, in both studies (Gugliotta et al., 2017; La Croix & Dashtgard, 2014) the locus of mud deposition occurs at the landward extent of the salinity intrusion; whereas in the Waihou River system, I have shown that is its located well before that, within an environment commonly subject to brackish water inundation. This result suggests that there may be subtle differences in the relative position of the TMZ between systems, but the broad trend is shown to be applicable to systems across a range of scales.

The most commonly encountered mud facies type in cores is thick structureless mud, Facies B, which constitute 47.5% of the classified mud beds. The mechanism for deposition of Facies B is fluid mud freezing to the bed under quasi-laminar plug flow conditions (Baas et al., 2009). The instrument data shows fluid muds form at the base of the channel, induced by flocculation at the toe of the saltwater-freshwater mixing front within the FMTZ, which are subsequently resuspended or washed seaward. The uppermost portions of core, as well as surface sediments are sandy, suggesting that most fluid muds aren't deposited in the base of channels. This observation could be due to multiple reason, including: 1) the deepest parts of channels are too energetic for long term presentation of fluid muds, and therefore fluid mud layers in cores reflect deposition at high positions in the channel profile, or 2) sandy material in the upper portions of cores may represent deposition over a short time period (i.e. event beds), and that the limited deployment duration has not allowed the observation of the full range of processes operating within the fluvial to marine transition zone (i.e. fluid mud preservation at the bed was not observed). Without geochronology on the sediments, the correct interpretation cannot be discerned. Dalrymple et al. (2003) noted that fluid mud layers were deposited in abundance at the base of fluvial tidal channels of the Fly River based on the observations of "freshly deposited" fluid muds in core. However, in this study there is no evidence to suggest that these fluid muds are well preserved in basal channel positions.

We see similar deposits in this modern system than those identified in the rock record and those described in flumes studies. The gradient of processes across the FMTZ results in a gradient of deposit types and is a predictor of longitudinal position across the FMTZ,

supporting the work of La Croix and Dashtgard (2015) who noted progressive changes in lithology and sedimentary structures (physical and biogenic) across the FMTZ in the Fraser River. In this study, I identified three of the four mud bed types that Mackay and Dalrymple (2011)'s study of the Bluesky Formation noted. However, the details of processes operating during deposition, as described by the flume studies of Baas et al. (2009) and Schieber and Southard (2009), were not captured in our study due to practical limitation in the data collection. However, we can speculate that the processes described in past flume studies are occurring within the study area based on the rapid clearing of the water column, and subsequent accumulation of material at the bed. The process of water clearing during fluid mud formation is complimented by the work of Wu et al. (2022), who noted similar instrument responses including the timing of processes with respect to the tidal cycle (just as the velocity approaches zero at slack tides).

2.5 Conclusion

For the first time, this study documents the range of depositional processes and their corresponding sedimentary response across the FMTZ in a modern river mouth system. Oceanographic instrumentation and co-located sediment data revealed the following process-response sedimentary characteristics within the lower Waihou River:

1) Peak mud deposition was found to occur in the middle of the study area (at approximately the neap tidal limit of the salinity intrusion) due to both depositional and preservational controls. The duration of brackish water mixing reduced towards the landward limit of the spring tidal salinity intrusion, limiting flocculation, and hence, deposition. Towards the mouth of the river preservation of mud deposits was limited as a result of fast tidal flow speeds.

2) The main type of mud identified in core was Facies B, thick structureless muds, interpreted to be the product of fluid mud deposition. Based on the lack of these beds in the upper sections of core, the low proportion of these muds recovered from channels in surface sediment surveys, and the observation of the repeated flushing of fluid muds from the bed in backscatter data, fluid muds seem to be poorly preserved at the base of channels. As a result, it is hypothesized that these fluid mud deposits accumulate higher in the cross-channel profile than previously thought.

3) Mud facies distribution is a good predictor of longitudinal position within the FMTZ. At the apex of deposition within the turbidity maximum zone, mud facies diversity was greatest, reflecting the complex mixture of fluvial and marine processes controlling mud deposition. However, at the most land and seaward end members mud facies diversity was extremely low, both exhibiting only one facies, which is likely a result of the dominance of riverine and marine processes, respectively.

The results of this study have important implications for interpreting near shore deposits in the sedimentary record, including the FMTZ in channels, which are known to hold economic quantities of hydrocarbons and other natural resources. This study can be used as a modern analogue for comparison and refinement of facies models, especially for rapidly deposited mud accumulations.

Chapter 3

Conclusions

The overall aim of this thesis was to improve depositional models for sedimentary deposits that accumulate in river channels through the fluvial to marine transition zone (FMTZ). This goal was achieved by comparing hydrodynamic conditions with co-located vibracores and surface sediment samples within the tidally influenced lower Waihou River in Aotearoa-New Zealand. The dataset allowed me to link trends in depositional processes with their corresponding sedimentary successions and surface sediment distributions. The distinct patterns recognised throughout the transition zone should be of great use to geoscientists seeking to better interpret nearshore environments in ancient strata (La Croix et al., 2019; Mackay & Dalrymple, 2011). Such improved interpretations and stratigraphic correlation within these shallow marine depositional settings are significant because they are known to contain substantial quantities of potable water and natural resources. Thus, a better understanding of how the sedimentary fabrics vary through space and time is essential to identify, extract, and manage these resources (La Croix et al., 2019; Mackay & Dalrymple, 2011; Weymer et al., 2020). This chapter focuses on directly responding to the research questions posed at the beginning of the study (in Chapter 1), and makes suggestions for further work.

Research Question 1: Can dynamically deposited mud be directly observed within a modern sedimentary system and the resultant deposits linked to the flow processes?

Figure 3.1 shows that fluid muds were successfully observed within the FMTZ of the Waihou River and that the distribution of these muds was linked to hydrodynamic processes. The fluid mud appeared to be the dominant control on the total proportion of mud deposited within the study area, and these deposits were greatest in the vicinity of Site 3 (Figure 3.1). Moreover, the fluid muds were found to be poorly preserved within the deeper portion of channels (and their deposits). This result is in contrast with observations from other systems in which fluid muds were found to accumulate in the base of channels (Dalrymple et al., 2003; Dalrymple & Choi, 2007). The precise reason for this difference should be explored in future work; however, possible explanations may lie in the particular tectonic setting of the Waihou, the

nature of the mixing front within the river, seasonal patterns in river flow, or timescales over which measurements were taken.

Near the most landward study sites in the Waihou River, the major control on net accumulation of sediment at the bed appears to be the duration of freshwater and brackish water mixing, and subsequently the amount of sediment flocculation. By contrast, near the mouth of the river, the dominant control on mud accumulation in the sedimentary archive is preservation (i.e., burial without erosion), which is a function of current velocity. I was able to deduce these controls on long-term mud accumulation by the tracking the movement of fluid mud layers using instrumentation, and by understanding the timing of the mixing and flushing of marine water within the system. Similar trends in mud deposition have been identified within other FMTZs globally (Gugliotta et al., 2017; La Croix & Dashtgard, 2014, 2015); however, the present study provides new insights into the reasons for these depositional patterns.

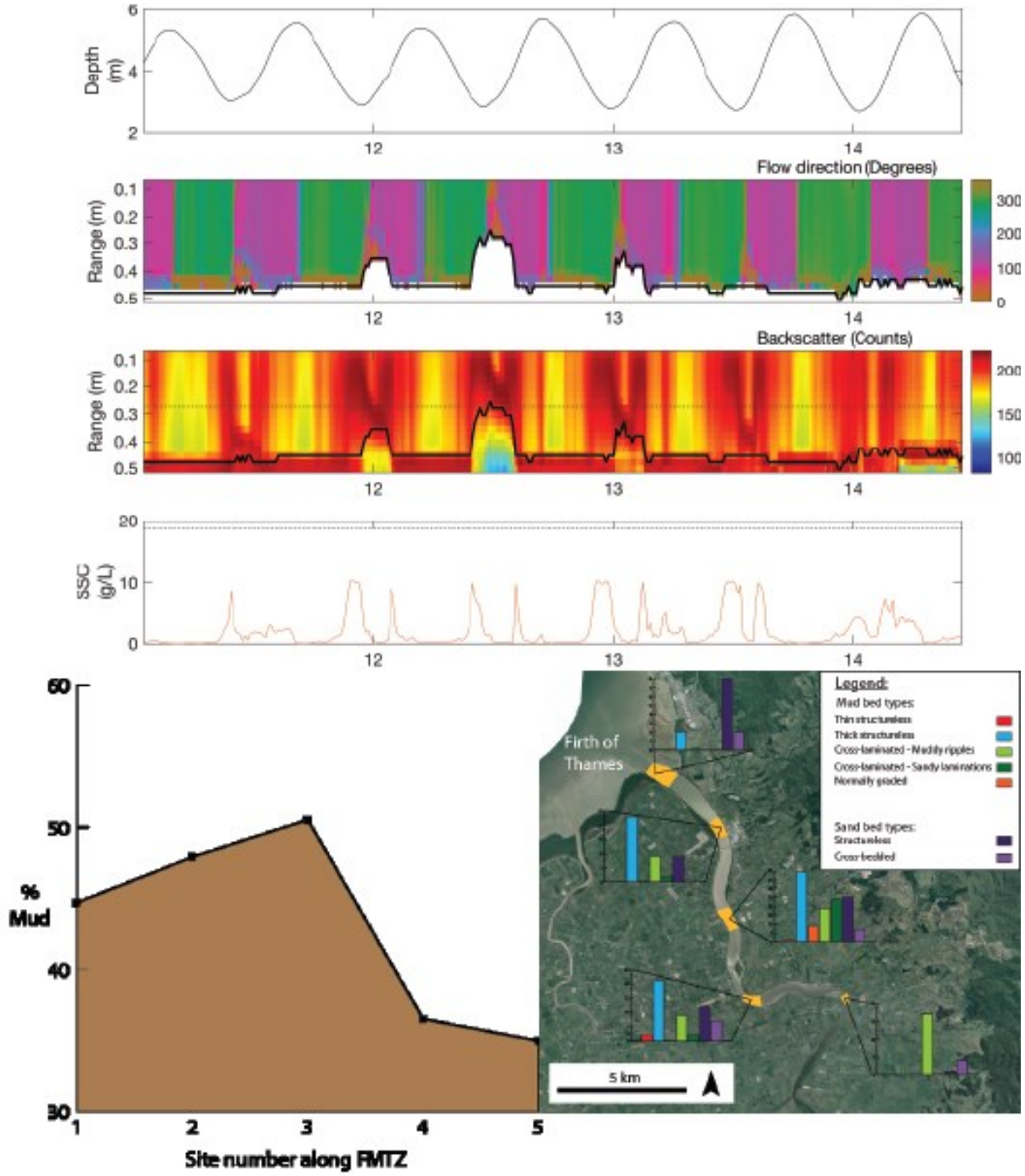

Figure 3.1 Summary of the main sedimentary processes, including formation of fluid mud (upper panel), and their depositional response such as proportion of mud (lower left panel) and mud facies type (lower right panel) observed across the FMTZ in the lower Waihou River, New Zealand.

Research Question 2: Can process-response relationships for mud be used to constrain depositional position along the FMTZ?

In addition to the proportion of total mud serving as an indicator of depositional position along the FMTZ, mud facies types were also shown to vary in a predictable manner (Figure 3.1). The greatest diversity in mud facies was observed in cores collected from Site 3, which is

considered to represent the variation in and relative strength of sedimentary process impacting sediment deposition; the central site is subject to the most variable process regime, having alternations between river and tidal dominance through neap spring cycles. The landward and seaward ends of the study area were distinctly different from Site 3, and displayed quite limited diversity in mud facies types, likely due to the strong dominance of river flow and tides, respectively (Figure 3.1). These trends in mud facies diversity will serve as a useful tool to estimate paleo-depositional position for other studies in the future.

Despite the marked success of this research project, there are a number of aspects that could be improved upon in future work. Ideally, I would deploy optical backscatter sensors (OBS) with a larger maximum turbidity range to capture the full range of observed suspended sediment concentrations (SSC). It would also be useful to obtain a vertical profile of SSC at multiple locations if possible. On top of changes to the instrumentation, a longer deployment period would provide a further indication of levels of variability within the system.

There are several additional data sets that could be used to test the interpretations made in this research, as well as to expand knowledge about freshwater-brackish water mixing dynamics, and allow more direct comparison of the stratigraphy present across the study area. Undertaking conductivity-temperature-depth transects throughout the FMTZ of the Waihou River might make it possible to determine whether mixing occurs within a salt-wedge, or if the water packages are well-mixed. Potentially, some of the subtle difference in sediment distribution between the Waihou River and other FMTZ's could be explained by differences in the nature of mixing. Geochronology of sediments, especially in the upper meter, would inform whether the sediments at the base of channels are event beds or, as hypothesised, that fluid mud deposits are poorly preserved within the deeper portions of channels. Investigation into the microstructure of mud beds may allow further subdivision of facies, giving a higher resolution picture of depositional position. Lastly, seismic surveys of the area would allow extrapolation of sediment architecture, yielding insights about how stratal thicknesses and continuity vary throughout the FMTZ.

Despite the challenging nature of the research, this study successfully links trends in hydrodynamic forcing to patterns in the resultant cored sedimentary successions through the FMTZ of a river. This initial study provides a foundation for future research in FMTZs, with the ultimate goal of building a workable depositional model of these complex, yet important sedimentary systems.

3.1 References

(AJHR) Appendix to the Journal of the House of Representatives. (1921). Waihou and Ohinemuri Rivers Commission (Report of), D-6F. *Government Printer*.

Baas, J. H., Baker, M. L., Malarkey, J., Bass, S. J., Manning, A. J., Hope, J. A., Peakall, J., Lichtman, I. D., Ye, L. P., Davies, A. G., Parsons, D. R., Paterson, D. M., & Thorne, P. D. (2019). Integrating field and laboratory approaches for ripple development in mixed sand-clay-EPS. *Sedimentology*, *66*(7), 2749-2768. https://doi.org/10.1111/sed.12611

Baas, J. H., & Best, J. L. (2002). Turbulence modulation in clay-rich sediment-laden flows and some implications for sediment deposition. *Journal of Sedimentary Research*, *72*(3), 336-340. https://doi.org/10.1306/120601720336

Baas, J. H., & Best, J. L. (2008). The dynamics of turbulent, transitional and laminar clay-laden flow over a fixed current ripple. *Sedimentology*, *55*(3), 635-666. https://doi.org/10.1111/j.1365-3091.2007.00916.x

Baas, J. H., Best, J. L., Peakall, J., & Wang, M. (2009). A phase diagram for turbulent, transitional, and laminar clay suspension flows. *Journal of Sedimentary Research*, *79*(3-4), 162-183. https://doi.org/10.2110/jsr.2009.025

Blott, S. J., & Pye, K. (2001). GRADISTAT: A grain size distribution and statistics package for the analysis of unconsolidated sediments. *Earth Surface Processes and Landforms*, *26*(11), 1237-1248. https://doi.org/10.1002/esp.261

Boehnert, S., Soto, S. R., Fox, B. R. S., Yokoyama, Y., & Hebbeln, D. (2020). Historic development of heavy metal contamination into the Firth of Thames, New Zealand. *Geo-Marine Letters*, *40*(2), 149-165. https://doi.org/10.1007/s00367-019-00597-9

Clement, A. J. H., Novakova, T., Hudson-Edwards, K. A., Fuller, I. C., Macklin, M. G., Fox, E. G., & Zapico, I. (2017). The environmental and geomorphological impacts of historical gold mining in the Ohinemuri and Waihou river catchments, Coromandel, New Zealand. *Geomorphology*, *295*, 159-175. https://doi.org/10.1016/j.geomorph.2017.06.011

Czarnecki, J. M., Dashtgard, S. E., Pospelova, V., Mathewes, R. W., & MacEachern, J. A. (2014). Palynology and geochemistry of channel-margin sediments across the tidal-fluvial transition, lower Fraser River, Canada: Implications for the rock record. *Marine and Petroleum Geology*, *51*, 152-166. https://doi.org/10.1016/j.marpetgeo.2013.12.008

Dalrymple, R. W., Baker, E. K., Harris, P. T., & Hughes, M. G. (2003). Sedimentology and stratigraphy of a tide-dominated, foreland-basin delta (Fly River, Papua New Guinea).

Dalrymple, R. W., & Choi, K. (2007). Morphologic and facies trends through the fluvial-marine transition in tide-dominated depositional systems: A schematic framework for environmental and sequence-stratigraphic interpretation. *Earth-Science Reviews*, *81*(3-4), 135-174. https://doi.org/10.1016/j.earscirev.2006.10.002

Dashtgard, S. E., & La Croix, A. D. (2015). Sedimentological trends across the tidal–fluvial transition, Fraser River, Canada: a review and some broader implications. *Developments in Sedimentology*, *68*, 111-126.

Dashtgard, S. E., Wang, A., Pospelova, V., Wang, P.-L., La Croix, A., & Ayranci, K. (2022). Salinity indicators in sediment through the fluvial-to-marine transition (Fraser River, Canada).

De Lange, P. J. (1989). *Late Quaternary development of the Kopouatai peat bog, Hauraki lowlands, and some palaeoenvironmental inferences* University of Waikato].

Dougherty, A. J., & Dickson, M. E. (2012). Sea level and storm control on the evolution of a chenier plain, Firth of Thames, New Zealand. *Marine Geology*, *307*, 58-72. https://doi.org/10.1016/j.margeo.2012.03.003

Folk, R. L., & Ward, W. C. (1957). Brazos River bar [Texas]; a study in the significance of grain size parameters. *Journal of Sedimentary Research*, *27*(1), 3-26.

Franklin, P., & Booker, D. (2014). *Flow regime requirements for instream ecology in the Waihou River catchment - Waihou catchment ecological monitoring 2009* (Waikato Regional Council Technical Report 2014/09, Issue. W. R. Council.

Gingras, M. K., Pemberton, S. G., Saunders, T., & Clifton, H. E. (1999). The ichnology of modern and Pleistocene brackish-water deposits at Willapa Bay, Washington: Variability in estuarine settings. *Palaios*, *14*(4), 352-374. https://doi.org/10.2307/3515462

Griffiths, G. A., & Glasby, G. P. (1985). Input of river-derived sediment to the New-Zealand continental-shelf .1. Mass. *Estuarine Coastal and Shelf Science*, *21*(6), 773-787. https://doi.org/10.1016/0272-7714(85)90072-1

Gugliotta, M., Saito, Y., Nguyen, V. L., Ta, T. K. O., Nakashima, R., Tamura, T., Uehara, K., Katsuki, K., & Yamamoto, S. (2017). Process regime, salinity, morphological, and sedimentary trends along the fluvial to marine transition zone of the mixed-energy Mekong River delta, Vietnam. *Continental Shelf Research*, *147*, 7-26. https://doi.org/10.1016/j.csr.2017.03.001

Hauck, T. E., Dashtgard, S. E., Pemberton, S. G., & Gingras, M. K. (2009). Brackish-water ichnological trends in a microtidal barrier island-embayment system, Kouchibouguac national park, New Brunswick, Canada. *Palaios*, *24*(7-8), 478-496. https://doi.org/10.2110/palo.2008.p08-056r

Healy, T. (2002). Chapter Fourteen Muddy coasts of mid-latitude oceanic islands on an active plate margin—New Zealand. In *Proceedings in Marine Science* (Vol. 4, pp. 347-374). Elsevier.

Hicks, D. M., Shankar, U., McKerchar, A. I., Basher, L., Lynn, I., Page, M., & Jessen, M. (2011). Suspended sediment yields from New Zealand rivers. *Journal of Hydrology (New Zealand)*, *50*(1), 81-142.

Hochstein, M., Tearney, K., Rawson, S., Davey, F., Davidge, S., Henrys, S., & Backshall, D. (1986). Structure of the Hauraki Rift (New Zealand). *Royal society of New Zealand bulletin*, *24*, 333-348.

Hochstein, M. P., & Nixon, I. M. (1979). Geophysical-study of the hauraki depression, North Island, New-Zealand. *New Zealand Journal of Geology and Geophysics*, *22*(1), 1-19. https://doi.org/10.1080/00288306.1979.10422550

Hogg, A. G., Lowe, D. J., & Hendy, C. H. (1987). University of Waikato radiocarbon dates I. *Radiocarbon*, *29*(2), 263-301.

Horstman, E. M., Lundquist, C. J., Bryan, K. R., Bulmer, R. H., Mullarney, J. C., & Stokes, D. J. (2018). The dynamics of expanding mangroves in New Zealand. In *Threats to Mangrove Forests* (pp. 23-51). Springer.

Houghton, B., & Cuthbertson, A. (1989). Geological map of New Zealand 1: 50,000, sheet T14 BD Kaimai. *Wellington, New Zealand, Dept. of Scientific and Industrial Research*.

Hunt, S., Bryan, K. R., Mullarney, J. C., & Pritchard, M. (2016). Observations of asymmetry in contrasting wave-and tidally-dominated environments within a mesotidal basin: implications for estuarine morphological evolution. *Earth Surface Processes and Landforms*, *41*(15), 2207-2222.

La Croix, A. D., & Dashtgard, S. E. (2014). Of sand and mud: Sedimentological criteria for identifying the turbidity maximum zone in a tidally influenced river. *Sedimentology*, *61*(7), 1961-1981. https://doi.org/10.1111/sed.12126

La Croix, A. D., & Dashtgard, S. E. (2015). A synthesis of depositional trends in intertidal and upper subtidal sediments across the tidal-fluvial transition in the Fraser River, Canada. *Journal of Sedimentary Research*, *85*(6), 683-698. https://doi.org/10.2110/jsr.2015.47

La Croix, A. D., Dashtgard, S. E., Gingras, M. K., Hauck, T. E., & MacEachern, J. A. (2015). Bioturbation trends across the freshwater to brackish-water transition in rivers. *Palaeogeography Palaeoclimatology Palaeoecology*, *440*, 66-77. https://doi.org/10.1016/j.palaeo.2015.08.030

La Croix, A. D., Dashtgard, S. E., & MacEachern, J. A. (2019). Using a modern analogue to interpret depositional position in ancient fluvial-tidal channels: Example from the McMurray Formation, Canada. *Geoscience Frontiers*, *10*(6), 2219-2238. https://doi.org/10.1016/j.gsf.2019.03.008

Leonard, G., Begg, J., Wilson, C., & Leonard, G. (2010). *Geology of the Rotorua area*. GNS Science Lower Hutt, New Zealand.

MacDonald, I. T., & Mullarney, J. C. (2015). A Novel "FlocDrifter" Platform for Observing Flocculation and Turbulence Processes in a Lagrangian Frame of Reference. *Journal of Atmospheric and Oceanic Technology*, *32*(3), 547-561. https://doi.org/10.1175/jtech-d-14-00106.1

Mackay, D. A., & Dalrymple, R. W. (2011). Dynamic mud deposition in a tidal environment: the record of fluid-mud deposition in the cretaceous bluesky formation, Alberta, Canada. *Journal of Sedimentary Research*, *81*(11-12), 901-920. https://doi.org/10.2110/jsr.2011.74

Macquaker, J. H. S., Bentley, S. J., & Bohacs, K. M. (2010). Wave-enhanced sediment-gravity flows and mud dispersal across continental shelves: Reappraising sediment transport processes operating in ancient mudstone successions. *Geology*, *38*(10), 947-950. https://doi.org/10.1130/g31093.1

Macquaker, J. H. S., & Bohacs, K. M. (2007). Geology - On the accumulation of mud. *Science*, *318*(5857), 1734-1735. https://doi.org/10.1126/science.1151980

Malarkey, J., Baas, J. H., Hope, J. A., Aspden, R. J., Parsons, D. R., Peakall, J., Paterson, D. M., Schindler, R. J., Ye, L. P., Lichtman, I. D., Bass, S. J., Davies, A. G., Manning, A. J., & Thorne, P. D. (2015). The pervasive role of biological cohesion in bedform development. *Nature Communications*, *6*, Article 6257. https://doi.org/10.1038/ncomms7257

Manville, V., & Wilson, C. J. N. (2004). The 26.5 ka Oruanui eruption, New Zealand: a review of the roles of volcanism and climate in the post-eruptive sedimentary response. *New Zealand Journal of Geology and Geophysics*, *47*(3), 525-547. https://doi.org/10.1080/00288306.2004.9515074

McBride, G., Reeve, G., Pritchard, M., Lundquist, C., Daigneault, A., Bell, R., Blackett, P., Swales, A., Wadhwa, S., & Tait, A. (2016). The Firth of Thames and Lower Waihou River. *Synthesis report RA2, coastal case study. Climate Changes, Impacts and Implications (CCII) for New Zealand to*, *2100*.

McCave, I. N. (1970). Depostition of fine-grained suspended sediment from tidal currents. *Journal of Geophysical Research*, *75*(21), 4151-+. https://doi.org/10.1029/JC075i021p04151

Mulder, T., Syvitski, J. P. M., Migeon, S., Faugeres, J. C., & Savoye, B. (2003). Marine hyperpycnal flows: initiation, behavior and related deposits. A review. *Marine and Petroleum Geology*, *20*(6-8), 861-882. https://doi.org/10.1016/j.marpetgeo.2003.01.003

Naish, T. R., Nelson, C. S., & Hodder, A. P. W. (1993). Evolution of holocene sedimentary bentonite in a shallow-marine embayment, firth-of-thames, New-Zealand. *Marine Geology*, *109*(3-4), 267-278. https://doi.org/10.1016/0025-3227(93)90065-4

Newnham, R. M., Delange, P. J., & Lowe, D. J. (1995). Holocene vegetation, climate and history of a raised bog complex, northern New-Zealand based on palynology, plant macrofossils and tephrochronology. *Holocene*, *5*(3), 267-282. https://doi.org/10.1177/095968369500500302

Potter, P. E., Maynard, J. B., & Depetris, P. J. (2005). *Mud and mudstones: Introduction and overview*. Springer Science & Business Media.

Pritchard, M., Swales, A., & Green, M. (2015). Influence of buoyancy-and wind-coupling on sediment dispersal and deposition in the Firth of Thames, New Zealand. Australasian Coasts & Ports Conference 2015: 22nd Australasian Coastal and Ocean Engineering Conference and the 15th Australasian Port and Harbour Conference,

Schieber, J., Southard, J., & Thaisen, K. (2007). Accretion of mudstone beds from migrating floccule ripples. *Science*, *318*(5857), 1760-1763. https://doi.org/10.1126/science.1147001

Schieber, J., & Southard, J. B. (2009). Bedload transport of mud by floccule ripples-Direct observation of ripple migration processes and their implications. *Geology*, *37*(6), 483-486. https://doi.org/10.1130/g25319a.1

Schieber, J., Southard, J. B., Kissling, P., Rossman, B., & Ginsburg, R. (2013). Experimental deposition of carbonate mud from moving suspensions: importance of flocculation and implications for modern and ancient carbonate mud deposition. *Journal of Sedimentary Research*, *83*(11-12), 1026-1032. https://doi.org/10.2110/jsr.2013.77

Schofield, J. (1960). Sea level fluctuations during the last 4,000 years as recorded by a chenier plain, Firth of Thames, New Zealand. *New Zealand Journal of Geology and Geophysics*, *3*(3), 467-485.

Shane, P., Black, T., & Westgate, J. (1994). Isothermal plateau fission-track age for a paleomagnetic excursion in the mamaku ignimbrite, New-Zealand, and implications for late Quaternary stratigraphy. *Geophysical Research Letters*, *21*(16), 1695-1698. https://doi.org/10.1029/94gl01576

Shanmugam, G. (1997). The Bouma Sequence and the turbidite mind set. *Earth-Science Reviews*, *42*(4), 201-229. https://doi.org/10.1016/s0012-8252(97)81858-2

Skinner, D. (1986). Neogene volcanism of the Hauraki volcanic region. *Royal society of New Zealand bulletin*, *23*, 21-47.

Sutherland, B. R., Barrett, K. J., & Gingras, M. K. (2015). Clay settling in fresh and salt water. *Environmental Fluid Mechanics*, *15*(1), 147-160. https://doi.org/10.1007/s10652-014-9365-0

Swales, A., Bell, R., Ovenden, R., Hart, C., Horrocks, M., Hermanspahn, N., & Smith, R. (2008). Mangrove habitat expansion in the southern Firth of Thames: sedimentation processes and coastal-hazards mitigation. *Environment Waikato technical report*, *13*.

Thornton, S. F., & McManus, J. (1994). Application of organic-carbon and nitrogen stable-isotope and c/n ratios as source indicators of organic-matter provenance in estuarine systems - evidence from the tay estuary, Scotland. *Estuarine Coastal and Shelf Science*, *38*(3), 219-233. https://doi.org/10.1006/ecss.1994.1015

Vundavilli, H., Mullarney, J. C., MacDonald, I. T., & Bryan, K. R. (2021). The interaction of buoyant coastal river plumes with mangrove vegetation and consequences for sediment deposition and erosion in a tidal environment. *Continental Shelf Research*, *222*, Article 104417. https://doi.org/10.1016/j.csr.2021.104417

Wang, A. H., Wang, Z. H., Liu, J. K., Xu, N., & Li, H. L. (2021). The Sr/Ba ratio response to salinity in clastic sediments of the Yangtze River Delta. *Chemical Geology*, *559*, Article 119923. https://doi.org/10.1016/j.chemgeo.2020.119923

Watton, G. (1995). *Taming the Waihou: the story of the Waihou Valley Catchment flood protection and erosion control scheme*. Waikato Regional Council.

Weymer, B. A., Wernette, P. A., Everett, M. E., Pondthai, P., Jegen, M., & Micallef, A. (2020). Multi-Layered High Permeability Conduits Connecting Onshore and Offshore Coastal Aquifers. *Frontiers in Marine Science*, *7*, Article 531293. https://doi.org/10.3389/fmars.2020.531293

White, P., Cameron, S., Kilgour, G., Mroczek, E., Bignall, G., Daughney, C., & Reeves, R. (2004). Review of groundwater in the Lake Rotorua catchment. *GNS Client Report*, *130*.

Wiles, P. J., Rippeth, T. P., Simpson, J. H., & Hendricks, P. J. (2006). A novel technique for measuring the rate of turbulent dissipation in the marine environment. *Geophysical Research Letters*, *33*(21), Article L21608. https://doi.org/10.1029/2006gl027050

Woodroffe, C. D., Curtis, R. J., & McLean, R. F. (1983). Development of a chenier plain, Firth of Thames, New-Zealand. *Marine Geology*, *53*(1-2), 1-22. https://doi.org/10.1016/0025-3227(83)90031-2

Wu, H., Wang, Y. P., Gao, S., Xing, F., Tang, J. P., & Chen, D. Z. (2022). Fluid mud dynamics in a tide-dominated estuary: A case study from the Yangtze River. *Continental Shelf Research*, *232*, Article 104623. https://doi.org/10.1016/j.csr.2021.104623